THE UNIVERSITY OF CALGARY

The Detection of Dwarf Mistletoe on Lodgepole Pine Using The Compact Airborne Spectrographic Imager (*casi*)

by

Andrew Stoness

A THESIS

SUBMITTED TO THE FACULTY OF GRADUATE STUDIES

IN PARTIAL FULFILLMENT OF THE REQUIREMENTS FOR

THE DEGREE OF MASTER OF SCIENCE

DEPARTMENT OF GEOMATICS ENGINEERING

CALGARY, ALBERTA

June 1996

THE UNIVERSITY OF CALGARY

FACULTY OF GRADUATE STUDIES

The undersigned certify that they have read, and recommend to the Faculty of Graduate Studies for acceptance, a thesis "The Detection of Dwarf Mistletoe on Lodgepole Pine Using the Compact Airborne Spectrographic Imager (casi)" submitted by Andrew Stoness in partial fulfillment of the requirements for the degree of Master of Science in Geomatics Engineering.

M. A. Chapman

Supervisor, Dr. M.A. Chapman
Department of Geomatics Engineering

Michael Collins

Dr. M.J. Collins
Department of Geomatics Engineering

Richard Revel

Dr. R.D. Revel
Faculty of Environmental Design

12 Sept. 1996
Date

ABSTRACT

Lodgepole pine dwarf mistletoe is a parasitic flowering plant affecting large stands of lodgepole pine in western Canada and the United States. Dwarf mistletoe causes serious economic losses in the Forestry sector by significantly reducing growth, causing deformed, unmarketable trees, and resulting in early mortality for many trees.

Present inventory methods are highly subjective and inaccurate. Long-term forest management plans are being developed based on Decision Support Systems (DSS). For these reasons, it is essential that more accurate inventory methods be developed. Airborne spectrographic imagers are being investigated by many researchers to determine their potential to provide this information.

A project was undertaken to study the applicability of the Compact Airborne Spectroscopic Imager (*casi*) for distinguishing between healthy and dwarf mistletoe infested lodgepole pine. A variety of *casi* bands, band combinations, and band transformations were evaluated for the purpose of discriminating between the healthy and mistletoe infested lodgepole pine. Classification results are presented and evaluated.

ACKNOWLEDGEMENTS

I would like to extend my thanks to my Supervisor, Dr. Mike Chapman, who surprisingly did not completely loose faith in me. I would also like to express my deepest gratification to my wife Karen Cameron who stood by me through this extended process. Paul Shepherd and John Miller are thanked for computer access which they provided the author in Toronto. Partial funding for this project was provided by Bow Crow Forest and Sun Pine Forest Products Ltd.

TABLE OF CONTENTS

LIST OF TABLES

LIST OF FIGURES

1. INTRODUCTION

1.1 THE PROBLEM: LODGEPOLE PINE DWARF MISTLETOE

Lodgepole pine dwarf mistletoe (*Arceuthobium americanum Nutt. ex Engelm.*) is a parasitic flowering plant affecting large stands of lodgepole pine (*Pinus contorta*) in western Canada and the United States. Dwarf mistletoe causes significant economic losses in the Forestry sector by significantly reducing growth, causing deformed, unmarketable trees, and resulting in early mortality for many trees.

1.2 PRESENT DWARF MISTLETOE INVENTORY METHODS

Two methods are currently being used by government agencies and forestry companies for dwarf mistletoe surveys. The predominant method at this time involves forestry staff producing sketch maps from airplanes or helicopters. The resulting sketch maps are digitized and entered into a Geographical Information System (GIS) and statistically extrapolated to provide estimates for the province's forested areas. This method relies on a visual analysis of the extent of dwarf mistletoe by a forestry expert flying over the forest and sketching infested areas on maps. As a result, this method is very subjective, and inherently, includes large sources of error. Various factors can have a large impact on the accuracy of the classification including changes in view angle, changes in sun angle, seasonal variations, a lack of reference trees, and the level of training and experience of the mapper. In addition, the resulting sketches are not well georeferenced and may result in large spatial errors if entered into a GIS or a decision support system (DSS).

The second inventory method involves the analysis of colour infrared aerial photographs. According to Reinartz (1993), studies have shown that large discrepancies exist between species inventories developed by different experts from the same aerial photographs. Classification agreement among a group of experts was reported to be only between 60 and 95%. The error in agreement was even larger when differentiating between different degrees of vegetation health. No absolute accuracy assessment was made since this was simply a comparison of classifications by a group of experts.

One potential method to reduce the classification error discussed above would be to digitize colour infrared images and analyse them in a remote sensing software package. There are, however, significant problems associated with this approach. An examination of colour infrared photography in the Department of Geomatics Engineering, at The University of Calgary, found that almost no difference could be visually detected between infested and clean stands of lodgepole pine, indicating that the potential for accurate classification using this approach is minimal (Chapman and Stoness, 1994). In addition, significant amounts of spatial and spectral information would be lost during digitizing, leading to a serious degradation in the quality of the images. A preferable approach would be to use an instrument which produces digital images directly. The resultant images could then be directly analyzed using image processing software and the results entered directly into a GIS or DSS.

Forest inventories and damage surveys are traditionally carried out on randomly sampled areas which are then statistically projected to the entire area of interest (Reinartz, 1993). Given all the errors inherent in the present system, the resulting inventories and surveys are often very inaccurate. Brandt and Amirault (1994) indicated that 4 main sources of error exist for Canadian forest surveys which are outlined below:

- Field survey methodology;
- Mapping and digitizing procedures;

- Lack of information on the impact of pests within the region;
- Inaccurate historical inventory data.

Their conclusion was that current estimates of forest damage were almost certainly underestimated due to a combination of errors from the above sources. Unfortunately, at the present time no method exists to determine the actual accuracy of the data.

Personal discussions with Alberta Forestry staff indicated that they are very concerned with the accuracy of such surveys (Personal discussion, 1995). The accuracy of surveys/inventories is becoming increasingly important with the development of DSSs for forest management. The results of models and forest-use scenarios are directly linked to the accuracy of the information input into the system. As a result, it is essential that more accurate inventory methods be developed to ensure the validity of forest management plans developed using DSSs.

1.3 REMOTE SENSING OF VEGETATION HEALTH

Remote sensing techniques have been used for analysing the health of vegetation for many years. Initially, due to the limitations of the available technology, remote sensing could only be used to determine widescale general indicators of vegetation health. Recent advances in multispectral and hyperspectral imagers with both high spectral and spatial resolution have greatly expanded the potential role of remote sensing in the analysis of vegetation health.

1.3.1 Spectral indicators of vegetation health

All objects absorb and reflect electromagnetic energy differently. As a result, the spectra of an object is similar to a fingerprint in that it is different for different objects. Variations in spectra is the main basis on which remote sensing relies for discriminating between objects.

The form of the vegetation spectra in the visible wavelengths of the spectrum is mainly due to the absorption characteristics of plant pigments, particularly chlorophylls *a* and *b*. Chlorophylls *a* and *b* absorb light energy in both the blue and red portion of the spectrum and reflect energy in the green wavelengths which gives healthy plants their characteristic green colour. In general, plants absorb 80 to 95 % of incident sunlight in the visible regions of the spectrum. The near-infrared (NIR) portion of the vegetation spectra is characterized by high levels of reflectance and low absorption of incident sunlight and is strongly influenced by internal leaf structure. Reflectance in the NIR is typically in the range of 40 to 50 % for healthy plants and this portion of the vegetation spectra is often termed the NIR plateau.

Stress induced by causes such as disease, pests, or incorrect moisture levels result in changes in plant physiology including variations in the concentrations of plant pigments and alterations in the physical structure of the plant leaves. These changes will be reflected in variations in the plant's spectra which can be detected using the appropriate remote sensing instruments. The general approach of remote sensing of vegetation health is to acquire spectra of the species of interest in a healthy state and compare this to the spectra of target plants to determine their health.

Generally, decreases in plant health have been found to cause a flattening of the spectral response with reduced reflection in the NIR and increased reflection in the visible portions of the spectrum. The reduction in the amount of reflection in the NIR plateau is caused by a breakdown in internal plant cellular structure which results in a decrease in the amount of leaf scattering (reflection). Changes or reductions in the concentration of pigments in the leaves (particularly chlorophyll *a* and *b)* cause increased reflection in visible wavelengths as chlorophyll absorption decreases. Studies which have reported these changes when studying stressed coniferous trees include Franklin and Raske (1994).

Deciduous trees undergo similar changes each fall in preparation for leaf drop. As the trees prepare for winter, the concentration of pigments in the leaves decreases which causes the leaves to generally change colour to brown or yellow as chlorophyll absorption decreases (Gunther, et al, 1994). In addition, the internal structure of the leaves breaks down and causes a reduction in reflectance in the NIR plateau. The net result is an overall flattening of the spectra similar to that found in unhealthy or stressed plants.

In some cases, stresses have been found to cause different responses than those discussed above. Essery and Morse (1992) found that the NIR reflection increased for Norway spruce which were exposed to ozone and acid rain pollution. The increased reflection was explained as being caused by an increase in the number of internal reflectance surfaces in the plant leaves caused by cells breaking apart. Similar increases in NIR reflection have also been found to result from both dehydration and the early stages of plant senescence (Essery and Morse, 1992). As a result of findings of this type, it is important to realize that high levels of NIR reflectance do not necessarily indicate good plant health. A study by Ekstrand (1994) found that image spatial resolution affects the resultant spectra which has important implications when choosing bands for different projects. Ekstrand found that for low resolution (Landsat TM - 30m x 30m) NIR wavelengths are highly correlated with defoliation and plant health with a decrease in NIR reflectance indicating decreased plant health and increased defoliation. The decrease in NIR reflectance was attributed to an increase in shadow within the stand as health decreased and defoliation increased. The increased contribution of bark to the spectral signature also contributed to the decrease in NIR reflectance.

In the case of high resolution *casi* imagery (spatial resolution equal to or smaller than tree crown size) Ekstrand (1994) found a much weaker correlation between a decrease in NIR reflectance and a decrease in plant health. Ekstrand also found a much stronger correlation between an increase in reflectance in visible bands with a decrease in plant health with the high resolution imagery. Ekstrand found that the strongest correlation with plant health and defoliation occurred in the red wavelengths. The differences in spectral response which were found in the high resolution imagery compared with lower resolution imagery were attributed to a decrease in the impact of shadowed areas (only pixels completely covering tree crowns were used in Ekstrand's study) combined with an increase in the contribution of variations in chlorophyll levels and an increase in the amount of bark visible in the high resolution imagery. Findings such as these indicate that optimal band selection will vary with spatial resolution and probably also with scene content.

Researchers have identified a number of specific indicators of plant health including the red edge, the RVI (ratio vegetation index), and the NDVI (normalized difference vegetation index). The "red edge" is the name which has been given to the region of the spectrum where reflection rises abruptly from the high absorption of the red wavelengths to the high reflectance characteristic of the NIR plateau (Held and Jupp, 1994). The red edge has been found to respond to changes in moisture levels, nutrients and stress by shifting toward the blue end of the spectrum (blue shift). This blue shift has been attributed to decreases in chlorophyll concentrations due to stress (Held and Jupp, 1994). The slope of the red edge has been found by several authors including Essery and Morse (1992) to be correlated with changes in plant health with a lower slope indicating decreased plant health. The lowering of the slope of the red edge would be consistent with the general premise of a flattening of the spectral response in unhealthy plants.

The ratio difference vegetation index (RVI) is a vegetation indice which is calculated by dividing NIR reflectance by red reflection to provide an indicator of plant health. This indice is based on the assumption that as plant health decreases, its NIR reflectance decreases while visible red reflectance increases. Thus this ratio is intended to highlight these changes with lower values indicating decreased vegetation health. The process of division also acts to remove the effects of factors such as topography and sun angle which act equally on all channels so that one type of object will appear the same regardless of differences in topography or sun angle (Hord, 1986).

The normalized difference vegetation index (NDVI) is another vegetation indice which has been widely used. The NDVI is very similar to the RVI in that a comparison of NIR and red reflectance is used, but it is calculated by dividing the difference between the NIR and red reflectances by the sum of the NIR and red reflectances.

Dwarf mistletoe may cause effects on lodgepole pine health which result in spectral changes similar to those discussed in this Section. It is this type of information which will be examined during this project in an effort to create a classification process which differentiates between healthy and dwarf mistletoe-infested lodgepole pine.

1.3.2 Other indicators of vegetation health

The spectral information discussed in Section 1.3.1 only takes into account a small amount of the total information which is available. For example, humans use much more information than the basic spectral information when viewing a scene including texture, pattern recognition, and context. Studies on coniferous forests conducted by several researchers including Ekstrand (1994) have indicated that at a spatial resolution of 0-5 meters, texture is often as important as spectral information in forest analysis. In the case of dwarf mistletoe-infested lodgepole pine, defoliation may cause a change in the texture of infested stands. As a result, several measures of texture will be calculated and analysed as input into the classification process along with the spectral information to determine whether this information improves classification accuracy.

1.4 The compact airborne spectrographic imager (*casi*)

The Compact Airborne Spectrographic Imager (*casi*) is an airborne pushbroom imaging spectrograph developed by ITRES Research Inc. of Calgary, Alberta. The *casi* is designed to image in the visible and near infrared wavelengths and has a sensitive range from 430nm to 870nm in the electromagnetic spectrum. For the project discussed in this paper, the *casi* was configured in a Spatial Mode which provides an image 512 pixels wide with up to 15 spectral bands. The spectral bands are programmable in 1.8nm increments. Details of the spatial resolution and the wavelengths of the bands used in this project will be discussed later in this paper. Further details of *casi* specifications can be found in a paper by Babey and Anger (1993).

The *casi* produces digital imagery which can easily be analysed in image processing packages. Once processed, this data is ideal for input into a DSS or GIS for further analysis. The programmable spectral bands of the *casi* allow data capture to be customized to highlight the particular phenomena of interest. The high spectral resolution (1.8nm) allows small changes to be detected in the spectra of plants. Another important feature of the *casi* is that the imagery can be accurately georeferenced. This is an extremely important feature if the data is to be included in a DSS. Another benefit of the *casi* is that it is a small, portable, low cost system which can be used to target areas in which dwarf mistletoe is suspected.

The medium spatial (1 to 10 meters) and high spectral resolution of the *casi* make it well suited for the analysis of vegetation health for forestry applications. The *casi* and other spectrographic imagers have been used over the past several years for various types of vegetation analysis due to its ability to detect small changes in plants caused by stresses such as water shortage or disease. Dwarf mistletoe causes stress, defoliation, and canopy changes in lodgepole pine. As discussed in Section 1.3.1, there should be noticeable changes in the spectral signature of infested trees such as a flattening of spectral response with an increase in visible reflection. NIR reflectance should also be affected, although studies by other authors are not consistent regarding the direction of the response. In the case of needle loss and canopy dieback the canopy should adopt a coarser texture.

The major goal of this project is to identify the best set of *casi* bands, band combinations, or band transformations for discriminating between healthy and dwarf mistletoe-infested lodgepole pine. The image analysis techniques which were used are discussed in later Sections of this paper.

1.5 Potential complicating factors

The basic nature of the forest poses difficulties for high resolution aerial remote sensing. The forest is a complicated mixture of plant communities. The information that is available increases greatly with increases in spatial resolution. Thematic Mapper (TM) or SPOT imagery pixels contain an average of all objects in the image over a 30 m^2 or 20 m^2 area, respectively and image pixels contain an average response from all objects in the pixel. In the case of mid or high resolution imagery, such as offered by the *casi* system, the situation is significantly more complicated. One pixel may contain 100% lodgepole pine while an adjacent pixel may contain a mix of understory and shadow. While the increase in information is extremely attractive, such imagery is much more difficult to analyze.

At spatial resolutions of less than 5m, the forest is a complicated mixture of trees, understory and shadows. In terms of the impact of shadows, when the resolution is less than about 5 meters, the image of a tree is composed of a sunlit crown and side and decreasing sun toward the shady side. In some cases, the forest floor will be exposed to sun while in most cases in a coniferous forest the forest floor will be in complete shade. Since forest companies are mainly interested in details on various tree species, it would be ideal if individual trees could be isolated from the rest of the data which is not required. Unfortunately, at the time of this project, automated tree isolation procedures were in the developmental stage and were not available for this project. Other methods for reducing the impact of shadows will be studied.

One potential approach to eliminate some of the above problems would be to obtain imagery during the winter season when the ground is snow covered to reduce the problems caused by understory. It may, however, be that the high response from the snow could wash out surrounding tree pixels making analysis impossible. This would of course only provide information on conifers as the deciduous trees would be void of leaves. If the snow is a significant problem, imagery obtained in the spring season before the leafout of understory plants would also be useful for conifer studies.

Another potential problem is that *casi* data may not allow for differentiation between different types of diseases. This could occur because different damaging agents can produce very similar symptoms to those caused by dwarf mistletoe including red needles, defoliation, and dead crowns. In addition, different diseases often exist on the same tree. This occurs because once a tree is weakened by one disease it is more susceptible to other diseases and pests. However, even if it is not possible to clearly differentiate between different diseases, the *casi* data would still allow for a detailed mapping of diseased trees and the highlighted areas could be further analyzed by fieldwork. An effort will be made to determine the impact of other diseases and pests on the study areas used in project. If the damage is determined to be mainly due to dwarf mistletoe, then the results of this study will provide data for future studies to determine whether dwarf mistletoe is differentiable from other diseases using remote sensing.

Site conditions such as soil type, moisture levels, slope and aspect can also have an impact on the health of lodgepole pine and their resultant spectra. As a result, efforts will be made to select a study site which has very consistent conditions in order to ensure that any spectral changes are due to dwarf mistletoe and not other factors. Future studies could study the impact of other factors on the accuracy of dwarf mistletoe classification.

Another complicating factor that other researchers have found is that in some cases the spectra of healthy specimens of one species look like unhealthy specimens of another species. Attempts will be made to reduce the impact of this sort of problem by the incorporation of ancillary information such as texture to augment the spectral information. This issue will be discussed further in Chapters 3 and 4.

1.6 RESEARCH METHODOLOGY

The purpose of this project is to evaluate the use of the *casi* for the identification and mapping of dwarf mistletoe (*Arceuthobium americanum*) on lodgepole *pine (Pinus contorta*). If the project is successful, this could provide a very valuable tool for all sectors of the forestry industry that are affected by dwarf mistletoe.

The following methodology was followed to meet the goals of this project:

1. Conduct ground-truthing to accurately characterize the study areas;
2. Examine the spectral characteristics of healthy and dwarf mistletoe-infested lodgepole pine to determine appropriate methods to differentiate between the two;
3. Determine which band ratios combinations, band ratios, and band transformations might improve the separation of infested and clean lodgepole pine and generate them;
4. Devise and conduct an optimization procedure to select the input for the classification process which will best distinguish between healthy and dwarf mistletoe-infested lodgepole pine using *casi* imagery;
5. Classify the imagery to maximize the distinction of dwarf mistletoe-infested lodgepole pine from healthy lodgepole pine;
6. Determine the accuracy of the classification of dwarf mistletoe infestation.

1.7 CONTRIBUTIONS OF THIS RESEARCH

Dwarf mistletoe causes significant damage to lodgepole pine stands in Western Canada. According to several authors, including Horsfall and Cowling (1977), dwarf mistletoe is one of the most serious threats to lodgepole pine in western Canada and the

United States and results in significant reductions in forestry yield in infested areas. Accurate, efficient assessment of the extent of dwarf mistletoe infestation is required to improve control. Present methods for assessment involve sketch mapping from aircraft or the analysis of colour infrared (CIR) photography. The first method relies on a visual analysis of the extent of dwarf mistletoe by a forestry expert flying over the forest and sketching infested areas on maps while the second method relies on a forestry expert visually classifying a CIR photo. As a result, both methods are very subjective and are not extremely accurate. In addition, the resulting maps of dwarf mistletoe infestation are not well georeferenced and are not appropriate for inclusion in a DSS. One factor which is repeatedly mentioned by researchers is the lack of accurate data on the extent of dwarf mistletoe infestation (i.e. Baker, 1992). The study described in this paper may provide a means for obtaining an accurate measure of the amount of trees affected by dwarf mistletoe.

Many forest companies are developing Decision Support Systems (DSS) to assist in better managing the forest resource. This type of system requires accurate, georeferenced data in order to provide accurate management information. *Casi* data could easily be integrated into a DSS for better analysis and management of mistletoe.

This project will provide an initial assessment of how well *casi* imagery can be used to discern between dwarf mistletoe-infested and clean lodgepole pine and will determine the best set of bands, band ratios, band combinations, and band transformations to maximize the separation. Results of this study will potentially benefit all sectors of the forestry industry which are plagued by losses due to dwarf mistletoe. As this is an initial study on the use of *casi* imagery for dwarf mistletoe detection, an effort will be made to ensure that dwarf mistletoe, and not other factors such as those discussed in Section 1.5, is the major cause of damage to the lodgepole pine in the study area. Future studies can build on the knowledge gained in this study to determine the impact of other factors on the accuracy of dwarf mistletoe classification. This work will also add to the general understanding of vegetation health assessment using remote sensing. In addition, the use of digital data, such as the *casi* imagery used in this study, may also assist in the assessment of factors which affect the viability and spread of dwarf mistletoe and could thereby contribute to the development of measures to control dwarf mistletoe.

1.8 THESIS OUTLINE

This thesis is divided into six chapters. The following Section briefly describes the content of each chapter.

Chapter 1 gives a general discussion of the issues relating to forest inventories and the need for improvements in data accuracy. Remote sensing of vegetation health and the remote sensing instrument used in this study are also discussed.

Chapter 2 offers a background discussion of lodgepole pine dwarf mistletoe. This discussion sets the stage for a detailed analysis of dwarf mistletoe infestation using *casi* imagery.

Chapter 3 contains a discussion of the study site in Kananaskis. Image processing operations and the generation of band combinations, band ratios, band transformations and other ancillary information are also discussed.

Chapter 4 covers the image classification process performed on the Kananaskis imagery, including a discussion of channel selection procedures, classification using the maximum likelihood classifier, and a discussion of the classification results.

Chapter 5 provides a summary of the research, conclusions, and recommendations for further research.

2. DWARF MISTLETOE

2.1 DWARF MISTLETOE

The many varieties of dwarf mistletoe are parasitic flowering plants from the family Loranthaceae which live on coniferous trees throughout a large portion of North America, particularly in north western Canada and the United States (Hiratsuka, 1987). According to Manion (1981), they are the most serious parasitic higher plants in North America. They result in serious economic losses and are among the most serious problems affecting western conifers including lodgepole pine, ponderosa pine, douglas fir, and western larch. In some areas of eastern Canada, black spruce is also severely affected. Economic losses result from reduced plant growth, premature death of trees, and lower quality products as a result of mistletoe infestation. Dwarf mistletoe also increases the vulnerability of infested trees to other diseases and pests. Approximately 20 species of dwarf mistletoe are found in North America (Horsfall, 1977) of which lodgepole pine dwarf mistletoe causes the most significant economic losses.

In this paper, only Lodgepole pine dwarf mistletoe will be studied. The purpose of this chapter is to provide background information on lodgepole pine dwarf mistletoe in order to obtain information to assist in developing a remote sensing-based technique for classifying dwarf mistletoe.

2.2 LODGEPOLE PINE DWARF MISTLETOE

Lodgepole pine dwarf mistletoe (*Arceuthobium americanum Nutt. ex Engelm.*) is the most prevalent dwarf mistletoe and the most serious in terms of economic impacts (Agrios, 1986). Lodgepole pine dwarf mistletoe is predominantly found on lodgepole pine *(Pinus contorta)* in western Canada and the northwestern United States, and on jack pine (*Pinus banksiana*) in eastern areas of Canada and the United States. It is also occasionally found on white spruce (*Picea glauca*), Scots pine (*Pinus albicaulis Engelm.*), ponderosa pine (*Pinus ponderosa*), and limber pine (*Pinus flexis*) (Hiratsuka, 1986).

2.2.1 Symptoms of dwarf mistletoe infestation

Although dwarf mistletoe results in serious reductions in plant growth and viability, the symptoms are often subtle and difficult to identify. Once dwarf mistletoe is established on a host, it interrupts the normal growth of the branch or trunk. At the point of infection, the tree becomes swollen and branches beyond that point become twisted and deformed and form clumps of branches called 'witches brooms'. Witches brooms are the most distinguishing symptom of mistletoe infestation. Other organisms, however, can also cause witches brooms so care must be taken to identify other more conclusive symptoms. The crowns of infested lodgepole pine become bunchy and discontinuous compared to the closed, smooth crowns of healthy trees. Dead and dying crowns are also indicators of heavy infestations of dwarf mistletoe. These symptoms can also be caused by other diseases or pest so it is often necessary to look for the most conclusive indicators of dwarf mistletoe which are aerial shoots or basal cups (Figure 2.1).

2.2.2 Life cycle

Dwarf mistletoe is a parasitic flowering plant which develops a root-like haustorium below the bark of its host. The haustorium develops sinkers which penetrate into the xylem of the host through which the dwarf mistletoe derives most of its carbohydrates and almost all of its water and mineral requirements (Manion, 1981). Three to five years after establishment on the host, greenish yellow aerial shoots, several centimetres in length, form in clusters around the infection point (Figure 2.1). After another one to two years, tiny yellowish flowers form on the aerial shoots in late spring or early summer. Dwarf mistletoe has separate male and female plants (dioecious) and seeds formed on the female plants produce dark berries which require about a year to ripen. Once the seeds are ripe, they are expelled over distances of up to 20 metres. The seeds are coated with a sticky viscous coating, called viscin, which allows them to stick to anything they strike. If a seed strikes a favourable host, it remains dormant until spring when it germinates and penetrates the bark of the host and the cycle repeats. Once the aerial shoots become inactive, they fall off exposing basal cups where they were attached to the host. As mentioned above, branch swellings and witches brooms can be caused by many other causes. Basal cups, therefore, are very important in positively identifying mistletoe as they remain for many years after the aerial shoots fall off.

Figure 2.1: Aerial shoots

In summary, the life cycle of dwarf mistletoe takes from 5 to 7 years from initial seed landing to seed production on a new host. After about 3 to 5 years, aerial shoots begin to appear and after another 1 to 2 years flower and seed production begins (Hiratsuka, 1987).

Due to the nature of its seed dispersal mechanism, dwarf mistletoe tends to occur in pockets of infestation which gradually expand outward in a radial pattern.

2.2.3 Extent of damage

Lodgepole pine dwarf mistletoe causes the largest disease or pest-inducted loss of productivity in lodgepole pine and jack pine. It is one of the most serious causes of economic loss in the forestry industry in western Canada and the northwestern United States (Hiratsuka, 1986).

Dwarf mistletoe absorbs water, carbohydrates and minerals from the host which causes deformities and reduced growth in the part of the branch beyond the infected area (Agrios, 1986). According to Agrios (1986), the dwarf mistletoe causes a hormonal imbalance of the host which results in swellings and twisted, contorted branch growths called witches brooms. The pathogen also reduces the vitality and growth of the entire tree. As the dwarf mistletoe develops, the areas of infestation deteriorate and become susceptible to attack by other diseases and pests. In addition, witches brooms often break off in wind storms creating further entry points for other pathogens.

Young lodgepole pine are most susceptible to serious damage from dwarf mistletoe as the disease affects their early growth. In addition, the pathogen then has a longer period over which to affect the tree such that many trees infected at a young age will never be suitable for harvest.

The severity of the infestation has a significant impact on the extent of visible indicators and on the extent of damage. Lightly infested trees may experience little loss of growth while severely infested trees will experience severe growth reductions and death. Forestry Canada estimates mistletoe causes an annual growth loss of approximately 4 million m^3 of wood in western Canada (Hall, 1994). Estimates however are not considered to be accurate and the actual amount could vary considerably. Researchers have reported that dwarf mistletoe can result in decreased growth of 30-60% in lodgepole pine (Steiner and Davidson, 1983).

In addition to reductions in growth, the damaged and deformed nature of heavily infested trees means that they may only be good for fire wood. Heavily infested stands also increase the risk of forest fires due to the presence of dead and dying limbs and crowns. In parks and other areas of public use, the unsightly appearance of infested trees is also a serious concern.

2.2.4 Potential indicators of dwarf mistletoe using remote sensing

In general, since dwarf mistletoe reduces the viability of lodgepole pine by absorbing nutrients and moisture, these changes should cause detectable changes in the spectra of infested trees. It can be hypothesized that a general flattening of the spectral response will occur with a decrease in green and NIR reflectance and an increase in reflectance in the blue and red portions of the spectrum. Since the tree limbs beyond the points of infection (witches brooms) are deprived of nutrients and water, significant variations should be evident in their spectra.

The resulting spectra will depend on the net contribution of all different impacts of the dwarf mistletoe. Field spectrometer measurements will be used to characterize the spectra of healthy and dwarf mistletoe-infested lodgepole pine to determine what differences, if any, actually occur.

The changes in canopy characteristics caused by dwarf mistletoe, including the creation of witches brooms, defoliation, and mortality should affect the texture of the forest canopy by decreasing crown closure. This should result in infested stands of lodgepole pine having a rougher texture compared to the high crown closure and resultant smoother texture of a healthy stand. Texture measures, therefore, will be considered during this project in an effort to augment the spectral data.

2.2.5 Control measures

At the present time, no chemical or biological controls exist for the management of dwarf mistletoe. Present control methods are limited to a combination of harvesting diseased trees which are reasonably healthy, and cutting and burning badly diseased trees. Due to the small distances that seeds are expelled, uninfested areas can be effectively protected by cutting buffer zones of at least 20 meters around infested areas. The planting of non-host species around infested areas is also recommended. It is particularly important to separate young stands as they are the most susceptible. Dwarf mistletoe has also been shown to spread by means of bird and animal vectors. Animal and bird vectors of mistletoe seed could potentially start new areas of infestation, but their impact is not controllable and is likely not important enough to consider when developing management plans. Studies by Punter and Gilbert (1989) concluded that bird and animal vectors were insignificant factors in the spread of dwarf mistletoe in Manitoba.

Under natural conditions, fire would effectively control dwarf mistletoe as lodgepole pine is a fire-dominant species which naturally rejuvenates because of periodic wildfires. Such fires would effectively control dwarf mistletoe because infested trees would be more susceptible to fire and burn more completely due to their damaged condition. Young lodgepole pine would have time to re-establish before dwarf mistletoe could become established again. However, for the last century, fire suppression has resulted in older forests in which dwarf mistletoe has not been controlled by fire. Many older stands are seriously infested with dwarf mistletoe due to the long period over which the parasite has had to spread. This condition is especially prevalent in Parks or other forest reserves where fire has been controlled and no logging or other control measures have been used.

2.2.6 Related research

Research is currently being conducted at the University of Manitoba and Utah State University into the biological requirements of dwarf mistletoe (e.g. Baker, Knowles and Slivitsky, 1982 and McQueen and Punter, 1994). The researchers are also developing a computer visualization model to model the spread of dwarf mistletoe to better understand how quickly it spreads and what factors affect the rate of spread. The ultimate goal of this research is the development of biological or chemical control methods for dwarf mistletoe.

One factor which is repeatedly mentioned by researchers is the lack of accurate data on the extent of dwarf mistletoe infestation (e.g. Baker, Knowles and Slivitsky, 1992). The study described in this paper may provide a means for obtaining an accurate measure or the amount of trees affected by dwarf mistletoe. In addition, the use of digital data, such as the *casi* imagery used in this study, may also assist in the determination of factors which affect the viability and spread of dwarf mistletoe and could contribute to the development of measures to control dwarf mistletoe.

2.2.7 Other lodgepole pine diseases

As mentioned previously, many of the symptoms of dwarf mistletoe can be caused by other diseases or pests. An effort was, therefore, made to ensure that the damage evident in the study areas was caused by dwarf mistletoe and not some other pathogen.

Table 2.1 summarizes other lodgepole pine diseases and pests and their significance in the study area.

A review of the Federal government's annual report on disease conditions entitled "Forest Insect and Disease Report" (Brandt, 1994), and discussions with forestry personnel indicated that no major outbreaks of other diseases or pests affecting lodgepole pine had occurred in the study areas recently. However, most of these surveys were done on a large scale from aircraft and it is possible that some other disease conditions do exist to a small degree. As mentioned previously, it is common for other disease agents to become established due to the weakened state of dwarf mistletoe infested trees and due to openings in the bark caused by witches brooms breaking off. Extensive ground truthing revealed that dwarf mistletoe is the major damaging agent affecting the trees in the study area.

Disease or pest	Comments
Atropellis canker	none in study areas
Climatic damage	possible
Mountain pine beetle	none in study areas
Lodgepole pine terminal weevil	none in study areas
Northern pitch twig moth	none in study areas
Pine needle casts	some observed in Bow Crow Forest
Stalaciform blister rust	high incidence in Banff & Jasper - none in study areas
Warren rootcollar weevil	none in study areas
Western gall rust	common throughout northwest region

Table 2.1: Lodgepole pine diseases and pests (Brandt, 1994)

Since many of the symptoms of dwarf mistletoe can be caused by other damaging agents, it is unclear whether the changes in spectral and textural characteristics of lodgepole pine caused by dwarf mistletoe are unique, or whether the impacts would be similar to the symptoms of lodgepole pine stressed by other diseases or pests. As this was an initial study on dwarf mistletoe, and no opportunity existed during the study to compare the effects of different damaging agents, future studies should look into this issue.

3. KANANASKIS STUDY AREA

3.1 STUDY AREA

The work for this thesis was focused on a study area located in the foothills of Alberta in Kananaskis Country near The University of Calgary Field Research Centre (Figure 3.1). Two data sets were acquired and analyzed for this site. The first data set was *casi* imagery and the second data set was field spectral data acquired using an Analytical Spectral Devices (ASD) Personal Radiometer II.

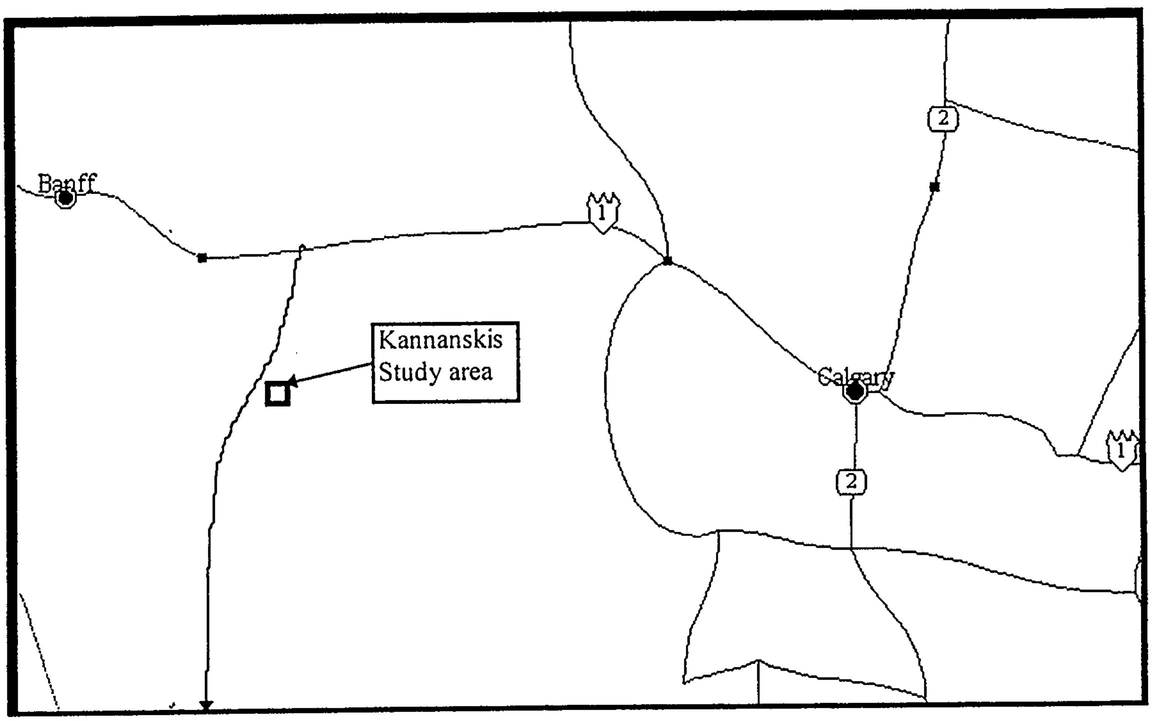

Figure 3.1: Study area location

The study area is located in a subalpine forest consisting mainly of stands of lodgepole pine and white spruce with some stands of aspen. The surrounding forest changes to subalpine fir and white spruce with increasing altitude. Most of the forest stands in the area are composed of relatively pure stands of each species. The Kananaskis study area was located following discussions with personnel from the Kananaskis Field Research Centre who indicated a general area where dwarf mistletoe was thought to exist. Subsequent field study located an area which had both stands of heavily dwarf mistletoe-infested as well as healthy lodgepole pine. An effort was made to ensure that conditions were very similar at both the infested and clean stands to ensure that any differences in spectra which might be detected were due to dwarf mistletoe and not due to other factors such as moisture stress. It was determined that conditions were very consistent and that the area was a good candidate for this project.

3.2 FIELD SPECTROMETER DATA AQUISITION

Field spectra were collected on September 16, 1995 with an Analytical Spectral Devices (ASD) Personal Spectroradiometer II. The field spectrometer measurements were obtained for two main reasons: to obtain a characterization of the spectral signatures of the major species in the study area (with an emphasis on the spectra of healthy and dwarf mistletoe-infested lodgepole pine); and for the creation of a reflectance image using a gravel road as a pseudo invariant object (Section 3.6.1).

3.2.1 Field spectra aquisition techniques

During the collection of field spectra, the spectrometer foreoptic was mounted on a survey tripod and was oriented so that it pointed vertically toward the ground where the targets were placed. All measurements were taken with a field of view of 18° and from a height of 1 meter which resulted in a field of view (FOV) of approximately 32 cm projected on the ground. All spectral measurements, except those taken of the gravel road, were taken over a brown reference blanket to eliminate contamination due to groundcover or surrounding objects (Figure 3.2). Samples were placed in a manner intended to both completely cover the reference blanket, and also to extend beyond the FOV of the sensor to ensure the capture of accurate spectra. For each reading a sample was used which was approximately 1m^2 in size and of a sufficient thickness to completely cover the brown reference blanket.

Conditions during the field spectrometer tests were sunny with a slight high haze and temperatures about 10°C. Samples of all objects of interest were collected including:

- aspen
- gravel road (pseudo-invariant object for creation of reflectance image)
- mature lodgepole pine
- mature lodgepole pine infested with dwarf mistletoe
- young lodgepole pine
- young lodgepole pine infested with dwarf mistletoe
- white spruce

Field spectrometer measurements were made for each object using the following methodology in order to help ensure accurate results:

1. A white reference measure was taken;
2. A dark current measure was taken;
3. Three raw spectra readings were taken from the object of interest and averaged into one raw sample value;

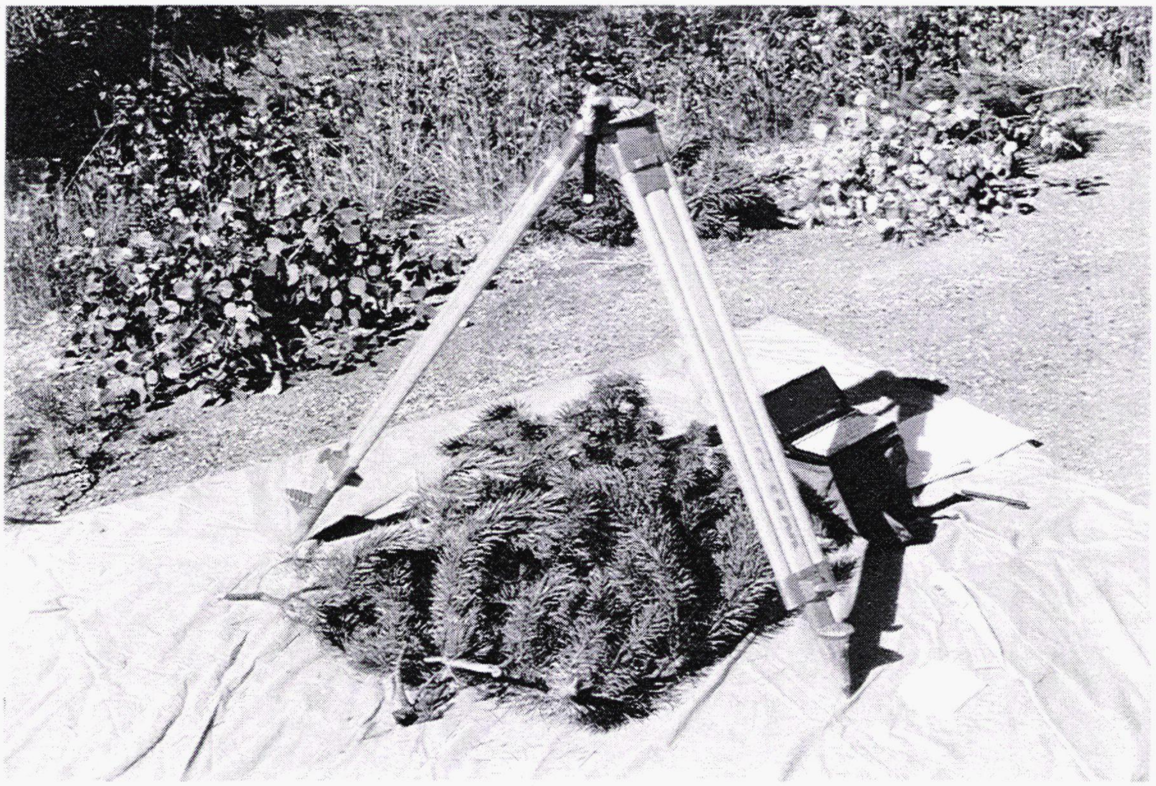

Figure 3.2: Field spectra collection

3.2.2 Field spectrometer data processing

The ASD field spectrometer was provided with processing software which will automatically create a spectra from the combination of a dark current reading, a white reference reading, and a raw object spectra reading. However, in order to preserve disk space, this process deletes the raw data files and replaces them with a single spectra file. Therefore, in order to avoid the potential loss of raw data due to errors in processing, raw measures of the white reference, dark current and object spectra were saved and post-processed, rather than use the real-time processing software.

The following procedure was carried out during field spectrometer data processing to obtain reflectance spectra for each object:

1. The dark current was subtracted from the raw object value;
2. The dark current was subtracted from the white reference;
3. The dark current-corrected white reference value was divided by the dark current-corrected raw object values to obtain reflectance spectra.

3.3 FIELD SPECTROMETER RESULTS

Following data processing, all spectra were entered into a spreadsheet software program and analyzed graphically to obtain a characterization of the different spectra and to provide information on what bands should be selected for dwarf mistletoe detection. In the following Sections, the spectra which were obtained are displayed and discussed.

3.3.1 Major tree species

Figure 3.3 shows the field-measured spectra of the major tree species in the Kananaskis study area. The results indicate significant differences between the major species which should permit accurate species-based classification. The largest differences were evident in the NIR plateau with all species widely separated in this portion of the spectrum. Significant differences were also seen across the visible portion of the spectrum. The smallest variation was found in the blue portion of the spectrum where there was little distinction between the major species. The high degree of separation between tree species is consistent with other research including a study by O'Connor, et al (1995). Based on the spectrometer results, classification schemes intended to differentiate between major tree species should include a combination of channels from the NIR plateau and the green and red wavelengths.

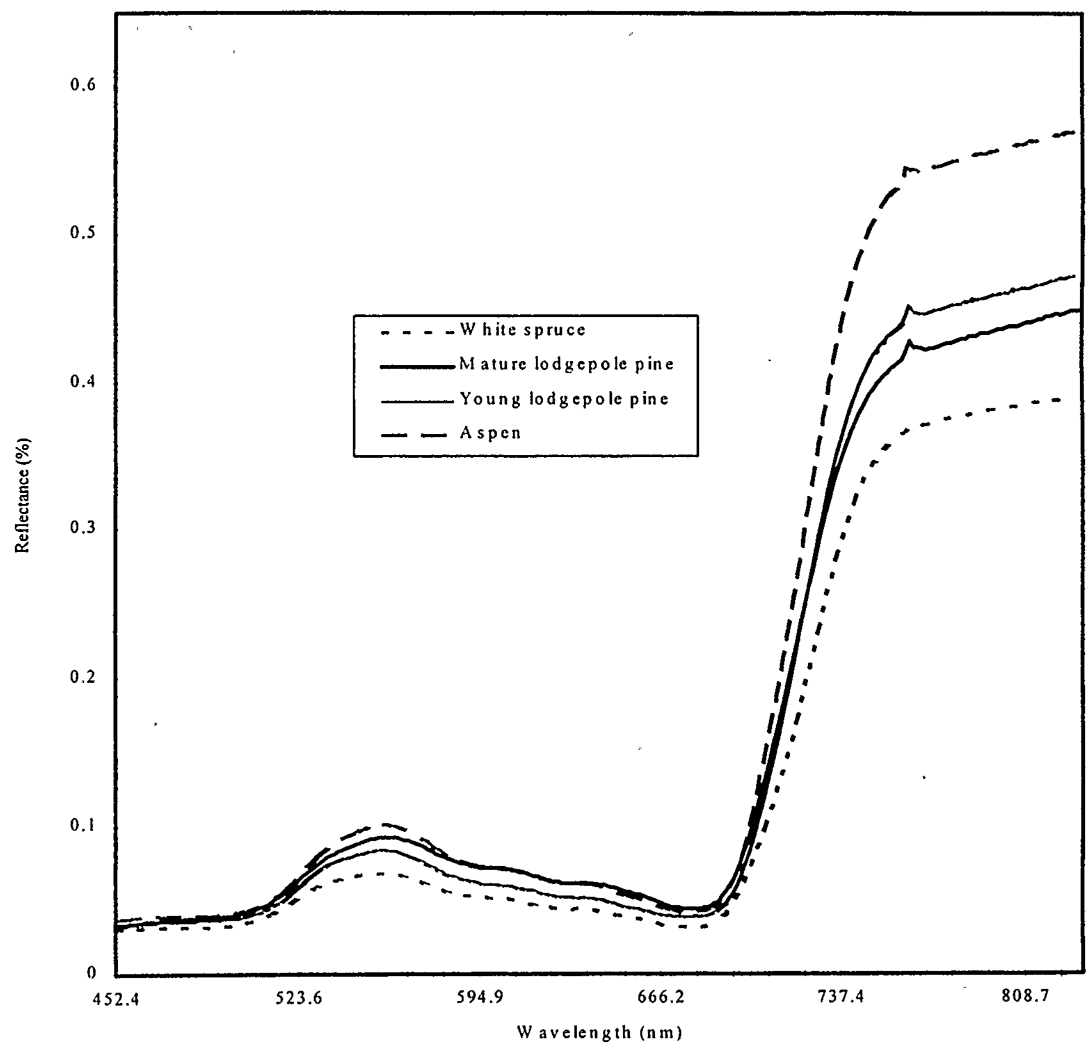

Figure 3.3: Spectra of major trees species in study area

3.3.2 Mature lodgepole pine

During the collection of lodgepole pine samples, it was noted that some trees had heavy coverings of pine cones which gave the trees a brown tinge of colour. As this could have an impact on the classification of lodgepole pine, a decision was made to determine the effects of pine cones on lodgepole pine spectra during the field spectrometer tests.

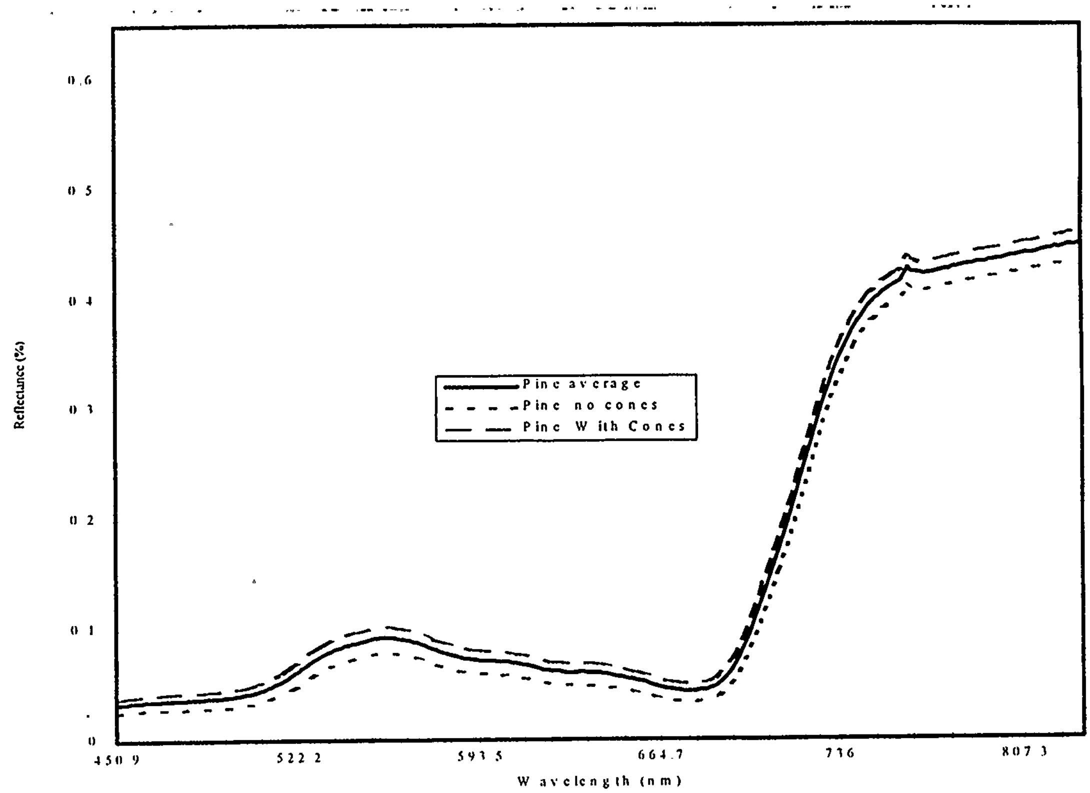

Figure 3.4: Effect of pine cones on the spectra of mature pine

Pine cones were found to have an impact on the spectra of healthy lodgepole pine. The effect of the pine cones was a higher reflectance in all portions of the spectrum for lodgepole pine with cones (Figure 3.4). The increased reflectance in the visible wavelengths can be explained by an increased reflectance due to the pine cones. The fact that pine cones had an impact on the mature lodgepole pine spectra implies that the season of multispectral image acquisition and the amount of pine cones present could have an impact on the mapping of lodgepole pine health status.

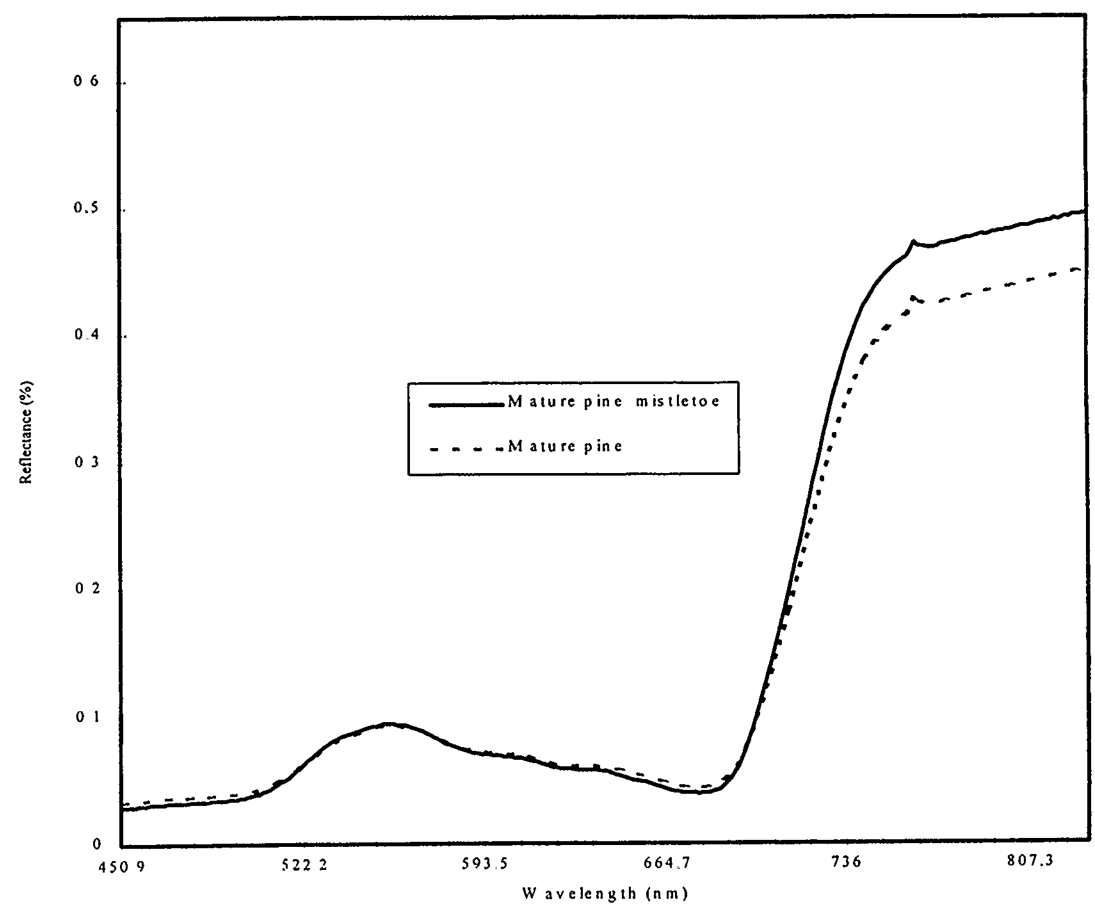

Figure 3.5: Spectra of healthy and dwarf mistletoe-infested mature lodgepole pine

For initial analysis, both classes of healthy lodgepole pine were averaged to produce one representative spectra for healthy mature lodgepole pine for comparison with dwarf mistletoe-infested lodgepole pine (Figure 3.5). This analysis revealed some differences between the two spectra, but no especially distinguishing spikes or differences in spectra were evident. The most significant difference was seen on the near-infrared plateau where the lodgepole pine with dwarf mistletoe exhibited a higher reflectance than the healthy lodgepole pine. The only difference evident in the visible wavelengths was a very slightly increased reflectance in the blue and red wavelengths for the dwarf mistletoe-infested lodgepole pine. Since the pine cones grow on the underside of the tree limbs it may be that they do not cause a considerable change in the tree spectra when the tree is viewed from above the canopy as it would be for the acquisition of the *casi* imagery. In order to study this, the spectra of the healthy lodgepole pine without pine cones was compared to the dwarf mistletoe-infested lodgepole pine spectra Figure 3.6.

Analysis of this comparison indicated significant differences between the two spectra. The dwarf mistletoe-infested lodgepole pine exhibited higher reflectance in all wavelengths which were sampled. The largest difference was again evident in the near-infrared wavelengths with infested lodgepole pine having a reflectance which was approximately 6% higher than the healthy lodgepole pine. Significant differences were also found in the visible wavelengths. The differences in the visible wavelengths were what would be expected for stressed vegetation, but again, the NIR reflectance was elevated which is the opposite to what is generally expected for stressed vegetation. A small blue shift of the red edge (approximately 5 nm) was also evident which has been correlated in other studies with decreased plant health (i.e. Essery and Morse, 1992).

This result is somewhat surprising in that most research suggests that stressed vegetation should exhibit an overall flattening of spectral response, with increased reflectance in the visible wavelengths and decreased reflectance in the NIR wavelengths (Held and Jupp, 1994). One possible explanation is that the field spectrometer readings were taken with the foreoptic focused too closely on the aerial shoots of the dwarf mistletoe and that the spectra are indicative of the spectra of the dwarf mistletoe itself and not of the stressed lodgepole pine. A more likely possibility, which was discussed in Section 1.3.1, was suggested in a study by Essery and Morse (1992) who found that the NIR reflection increased for Norway spruce which were exposed to ozone and acid rain pollution. The increased NIR reflection was explained as being a result of an increase in the number of internal reflectance surfaces in the plant leaves caused by cells breaking apart. Similar increases in NIR reflection have also been found to result from both dehydration and the early stages of plant senescence (Essery and Morse, 1992). The elevated NIR reflectance in the dwarf mistletoe-infested lodgepole pine could have been caused by the dwarf mistletoe restricting water flow to the infested branches which could cause an effect similar to that found by Essery and Morse (1992).

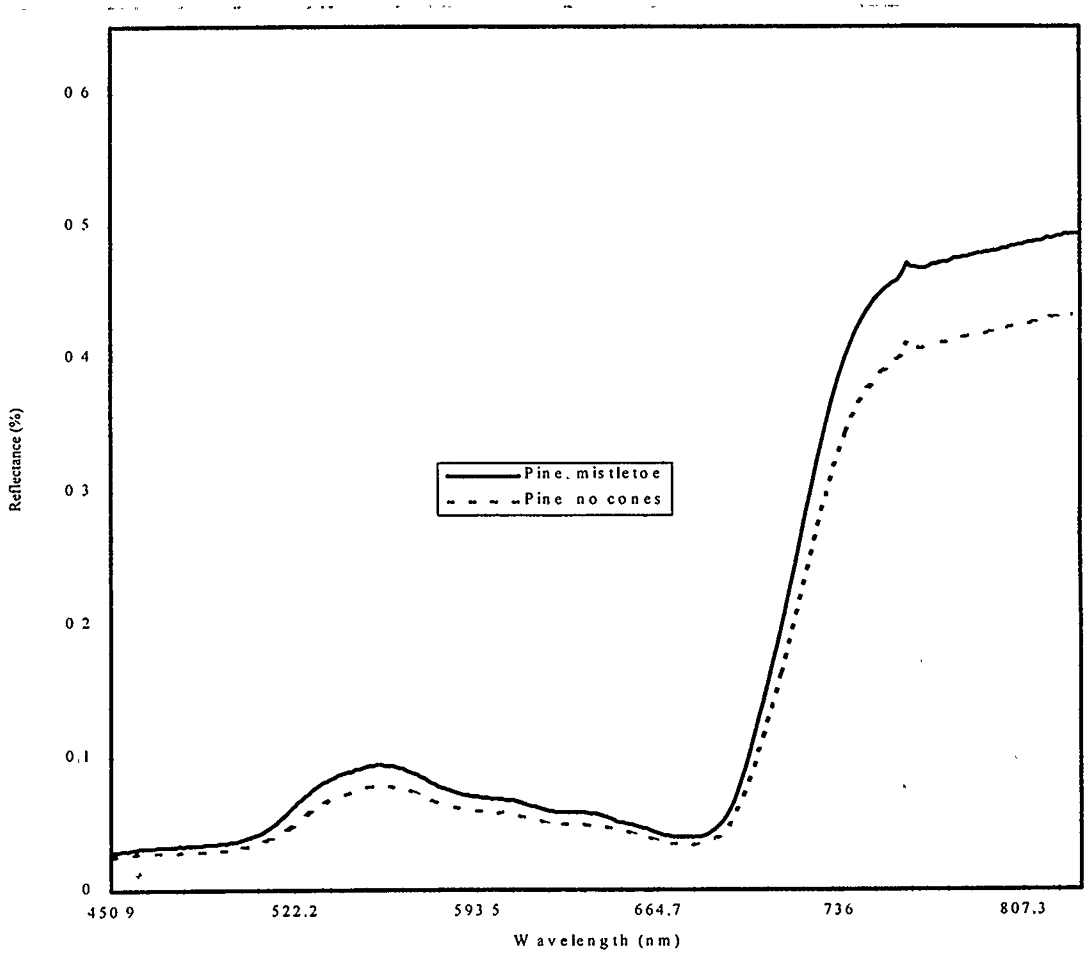

Figure 3.6: Healthy lodgepole pine without cones and mistletoe-infested pine

No especially distinguishing spikes or radical differences were found at any particular wavelength which indicates that a single defining band does not exist and that a combination of information from different wavelengths will be required to distinguish between healthy and dwarf mistletoe-infested lodgepole pine using the *casi.* This is in agreement with Leckie (1992) who suggested that it is unlikely that any "magical" bands will be found to provide extremely accurate classification in a forest environment. Based on the analysis of the field spectrometer results, band selection for a classification intended to differentiate between healthy and dwarf mistletoe-infested lodgepole pine should emphasize the NIR wavelengths (750-850nm) and the peak of green reflectance (~550nm). Additional channels should be selected from the area of the spectrum between the upper portion of the green wavelengths and the middle portion of the red wavelengths (550-650nm) as well as the lower portion of the green wavelengths (500-550nm), both regions in which small differences were evident in the field spectra of lodgepole pine.

3.3.3 Young lodgepole pine

Large differences were evident between the field-measured spectra of healthy and dwarf mistletoe-infested young (< 10 years old) lodgepole pine (Figure 3.7). The spectra of the infested young lodgepole pine showed a decrease of over 10% in near-infrared reflectance, a slightly lower reflectance in the green wavelengths, and small increase in red reflectance. The differences are consistent with the findings of other studies regarding the spectral response of plants to stress (i.e. Ashrar, 1989) and indicate that it should be possible to separate the two classes using spectral information. Based on these findings, band selection for the purpose of differentiating between healthy and dwarf mistletoe-infested young lodgepole pine should place an emphasis on the near-infrared plateau. Additional channels should be selected from the red wavelengths and near the peak of green reflectance (~550nm).

Due to the small size of the young lodgepole pine, image spatial resolutions of less than 1 meter would be required to accurately differentiate between the two states of young lodgepole pine and therefore no attempt will be made using the 2.5 meter imagery used for this study. The potential exists for future studies to detect dwarf mistletoe at a very young age which would allow for forestry companies to take appropriate measures such as destroying the young trees and replanting after removing the source of the dwarf mistletoe.

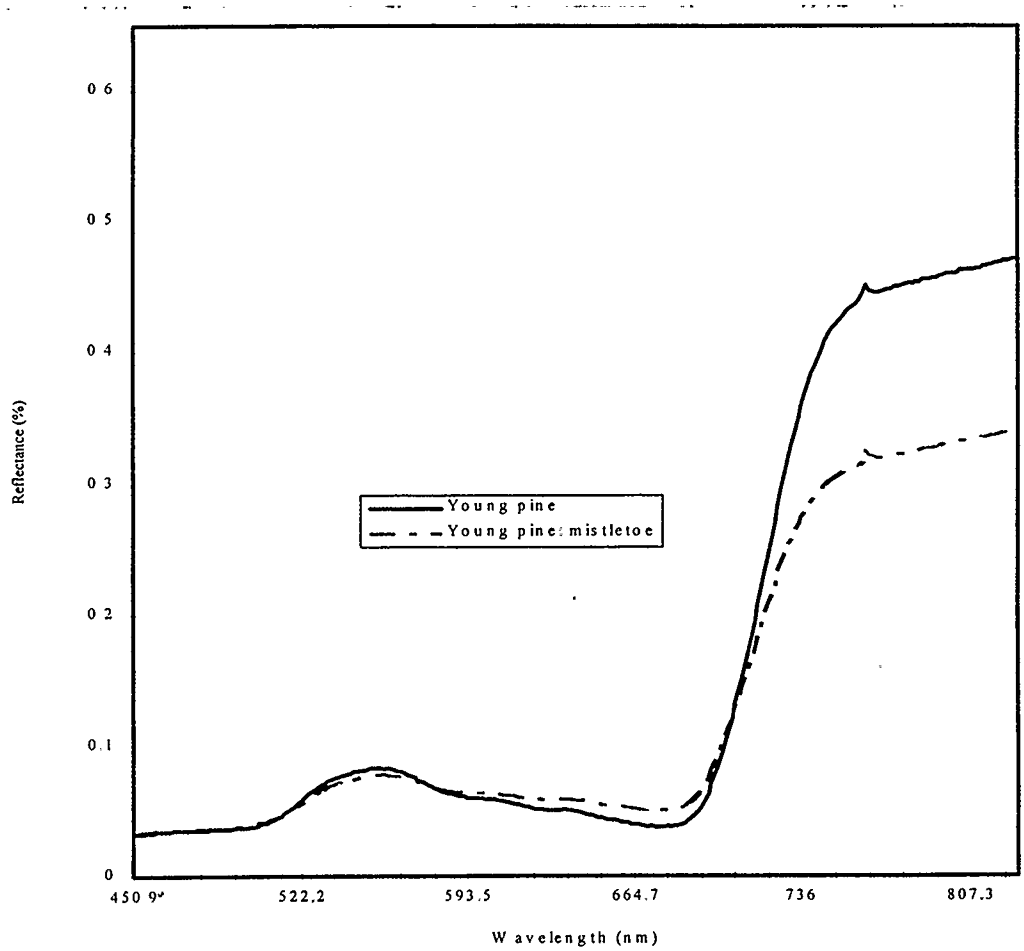

Figure 3.7: Young lodgepole pine spectra

3.3.4 Aspen

An analysis of field-measured aspen spectra revealed large variations between the spectra of green aspen and aspen yellowing due to seasonal effects (Figure 3.8). The differences included a large decrease in near-infrared reflectance and significant increases in reflectance from all visible portions of the spectrum. The large spectral differences would be caused by changes in leaf pigment concentrations including decreased chlorophyll levels which would result in decreased chlorophyll absorption and a colour change in the leaves. The large variation in aspen spectra due to seasonal effects indicates that the fall season is not an appropriate time for conducting forest surveys of deciduous plants with multispectral scanners.

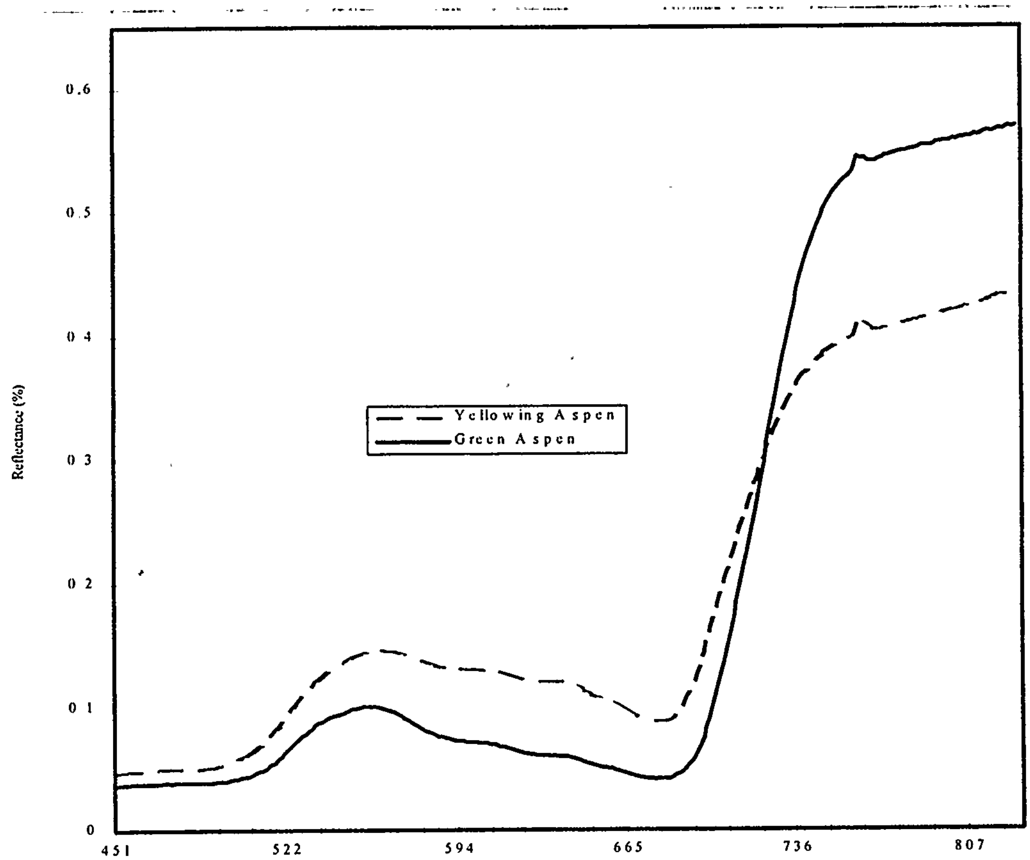

Figure 3.8: Aspen spectra

3.4 AIRBORNE SPECTROMETER TEST

Spectrometer measurements were taken from a helicopter on September 13, 1996. The purpose of obtaining the spectra from a helicopter was to compare the results to the field spectra obtained using the same ASD Spectroradiometer II which was used in the ground tests. As a result of the helicopter spectra being taken from above the canopy, the spectra should be more representative of the image obtained by the *casi.* However, studies by Milton, et al (1994) indicated that viewing angle is an extremely important factor when obtaining spectra. They found that large variations in spectra can result from varying the viewing angle. In order to produce somewhat standardized spectra, an attempt was made to obtain all spectra from the sunlit side of tree canopies with the sensor foreoptic aligned on a consistent angle from the vertical. It should be understood that it was impossible to maintain a consistent viewing angle and that the resultant spectra may not be accurate. The elevation of the helicopter was held reasonably constant during the aquisition of each set of spectral readings at a height of approximately 10 meters above the canopy. However, no method was available to accurately determine the height and it is assumed that the height actually varied from approximately 5 to 15 meters. Based on this assumption, the spatial resolution of the spectrometer would have varied from approximately 1.8 to 5 meters in diameter which is similar to the the spatial resolution of the *casi* imagery used in this study (2.5 meters).

3.4.1 Results of the helicopter spectrometer test

A review of the spectra obtained from the helicopter found considerably different results from those obtained during the field tests with the tripod.

Figure 3.9 shows the spectra of mature lodgepole pine obtained from both the helicopter and from the ground. While the dwarf mistletoe-infested lodgepole pine exhibited higher reflectance than the healthy lodgepole pine as was seen in the field tests, the spectra from the helicopter had significantly lower reflectance values in all portions of the spectrum. The lower reflectance levels obtained from the helicopter are probably due to a number of factors including the low sun angle caused by the time of acquisition (9:30 A.M.) and the nature of the lodgepole pine tree crowns. The structure of the mature lodgepole pine crowns is such that with the low sun angle, illumination conditions were created in which small sunlit crown tops were surrounded by large areas of shadow. The movement of the helicopter made it difficult to focus on the tree tops and, as a result, the spectra probably contained significant input from shadowed areas.

The spectra which was obtained from the helicopter of heavily infested lodgepole pine which were dead and dying had the form which would be expected - an overall flattened spectra with lower NIR reflectance and higher reflectance in the visible wavelengths indicating decreased plant health. As discussed above, the spectra from the helicopter were significantly reduced in value across the entire spectrum with values in the order of approximately 50 % of the reflectances obtained from the ground tests. This reduction can be explained as being a result of a combination of increased shadow caused by the low sun angle and inaccurate target lock. Additional variation could have been caused by variations in the view angle due to helicopter movement and distortions caused by turbulence from the helicopter which caused a large amount of movement in the needles which would have effects similar to changing the viewing angle.

As with the ground tests, no especially distinguishing spikes or radical differences were found at any particular wavelength which indicates that a single defining differences does not exist and that a combination of information from different wavelengths will be required to distinguish between healthy and dwarf mistletoe-infested lodgepole pine using the *casi.*

In terms of band selection for the purpose of differentiating between healthy and infested mature lodgepole pine, the spectra obtained from the helicopter indicated the same general differences in spectra as were shown by the ground tests. There was again a

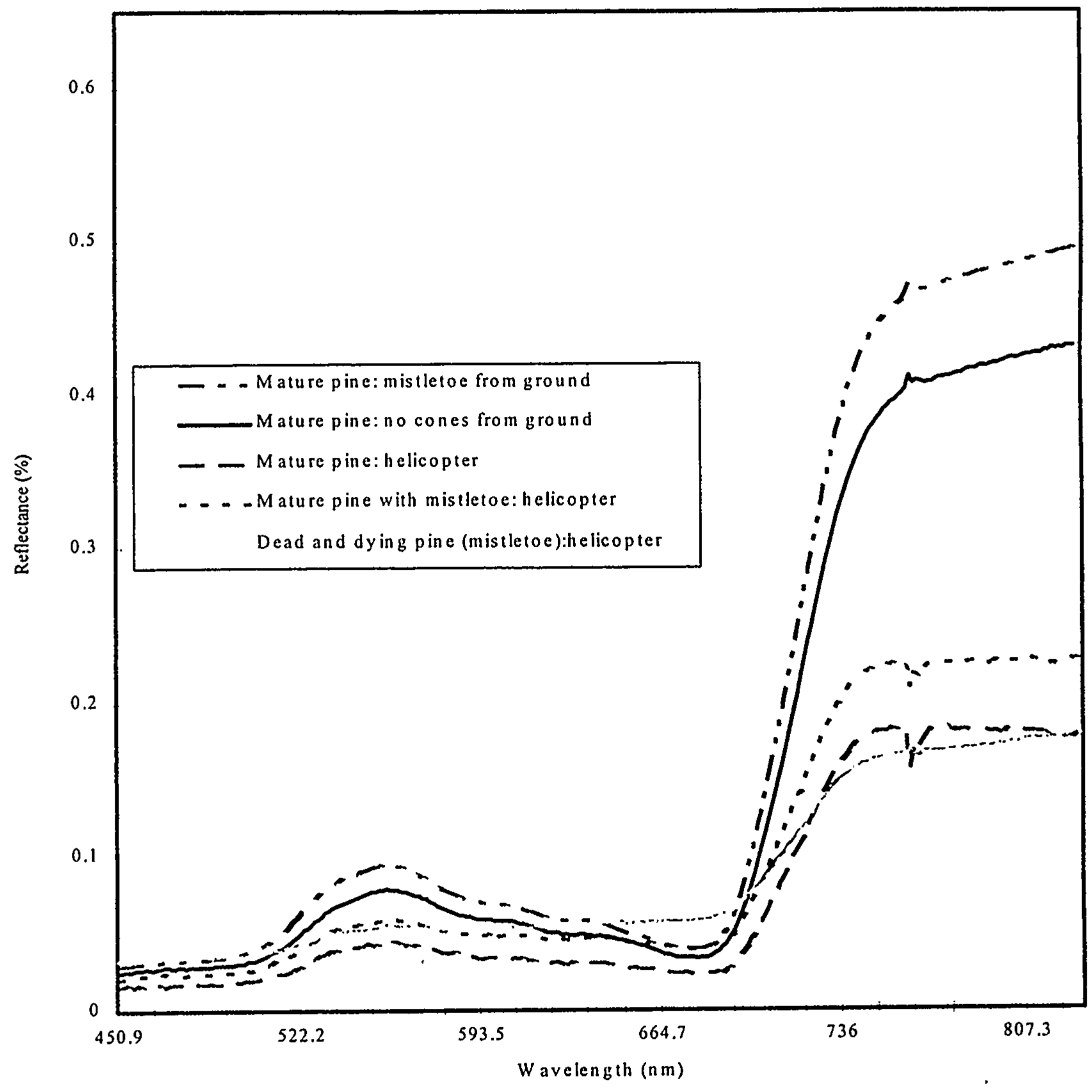

Figure 3.9: Mature pine spectra from helicopter

significant difference between the spectra in the near-infrared portion of the spectrum indicating that channels in this region should be emphasised.Differences were also evident in the visible portion of the spectrum from the upper portion of the blue wavelengths through to the red edge indicating that channels should be selected from across this range. The spectra from the helicopter indicated a larger blue-shift of the red edge (approximately 10 nm) indicating that a channel should be selected from this range (700-730nm).

Figure 3.11 shows the spectra of young lodgepole pine and mature white spruce acquired from both the helicopter and the ground. The differences which were evident in the spruce spectra were very similar in nature to those evident in the mature lodgepole pine spectra with much lower reflectance levels in the helicopter-obtained spectra. As with the mature lodgepole pine, the low reflectance levels were probably caused by the large amount of shadow which was present. The young lodgepole pine spectra exhibited differences which were considerably different than those observed with the mature lodgepole pine and spruce. The young pine spectra obtained from the helicopter had higher reflectance than the spectra acquired from the ground. The young pine stands had much lower levels of shade because the stands were very dense and similar in height which resulted in a more uniform illumination and a resultant larger target area. This would explain the fact that the spectra from the helicopter did not exhibit the low reflectance levels of the mature pine and spruce. The fact that the helicopter-acquired spectra had higher reflectance than those obtained from the ground may possibly be due to turbulence from the helicopter blades. During the test, it was observed that the needles were fluttering and moving from the wind which could explain some the differences observed especially if the needles were being turned over so that the lighter-coloured underside of the needles was exposed to the sensor.

The aspen spectra obtained from the helicopter are shown in Figure 3.11. As with the young lodgepole pine, the stands of aspen were much more uniformly illuminated than the mature stands of lodgepole pine and spruce and had reflectance levels in the same range as those acquired from the ground. The aspen spectra acquired from the helicopter, however, did exhibit significant differences from those obtained from the ground. The reflectance in the visible wavelengths, particularly in the green portion of the spectra, was much higher than the spectra acquired from the ground tests which is

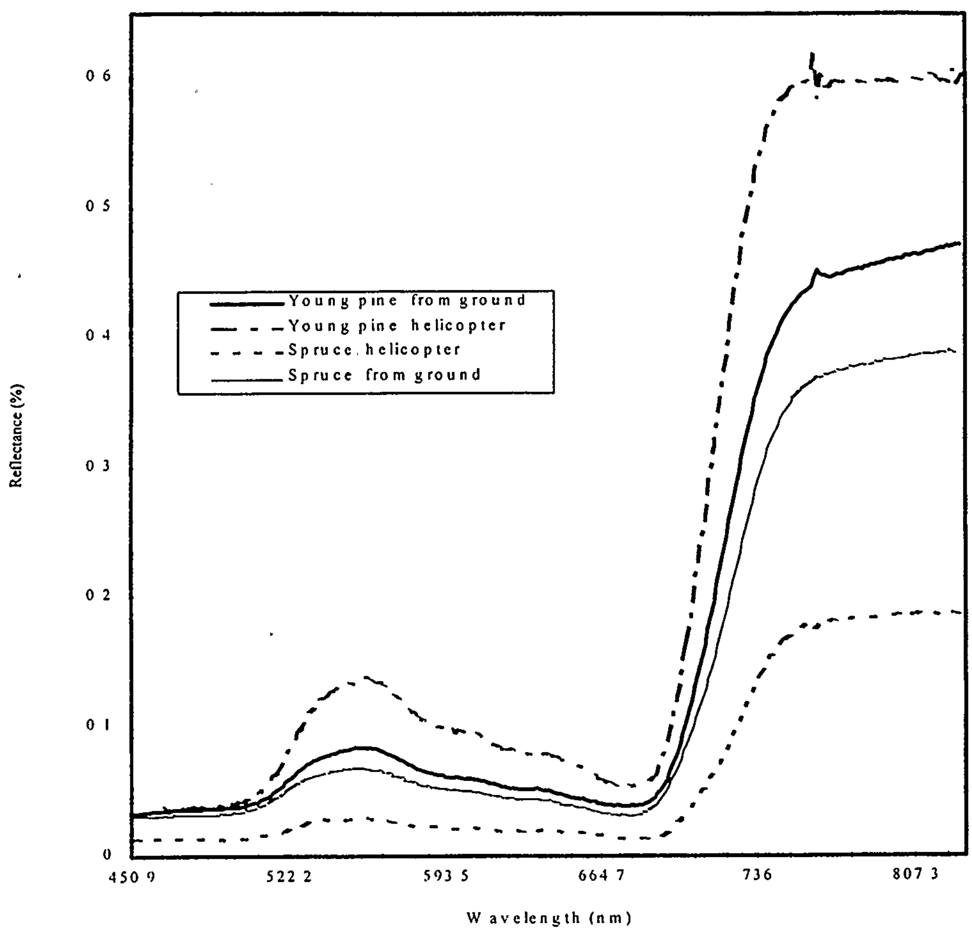

Figure 3.10: Young pine and mature white spruce spectra from helicopter

difficult to explain. As with the young lodgepole pine, some of the variation may be due to turbulence caused by the helicopter which was hovering very close to the canopy and causing significant leaf movement.

3.4.2 Benefits of helicopter tests

The main benefits of the helicopter experiment were purely academic. It quickly became apparent that the process was not as simple as envisioned as many problems quickly emerged. One of the biggest factors was that a helicopter is not a stable platform and as a result, it is very difficult to maintain an accurate lock on a target. The result of this was that spectra obtained from a helicopter probably consist of a mixture of a larger area than intended and thus may not be the pure spectra of the target. This is extremely important when dealing with mid and high-resolution imagery (< 5 meters) due to the rapid variations which exist between the canopy and surrounding shadow and understory. It was evident from looking down at the canopy from the helicopter that large variations in spectra would be caused by shadows in mid or high-resolution imagery.

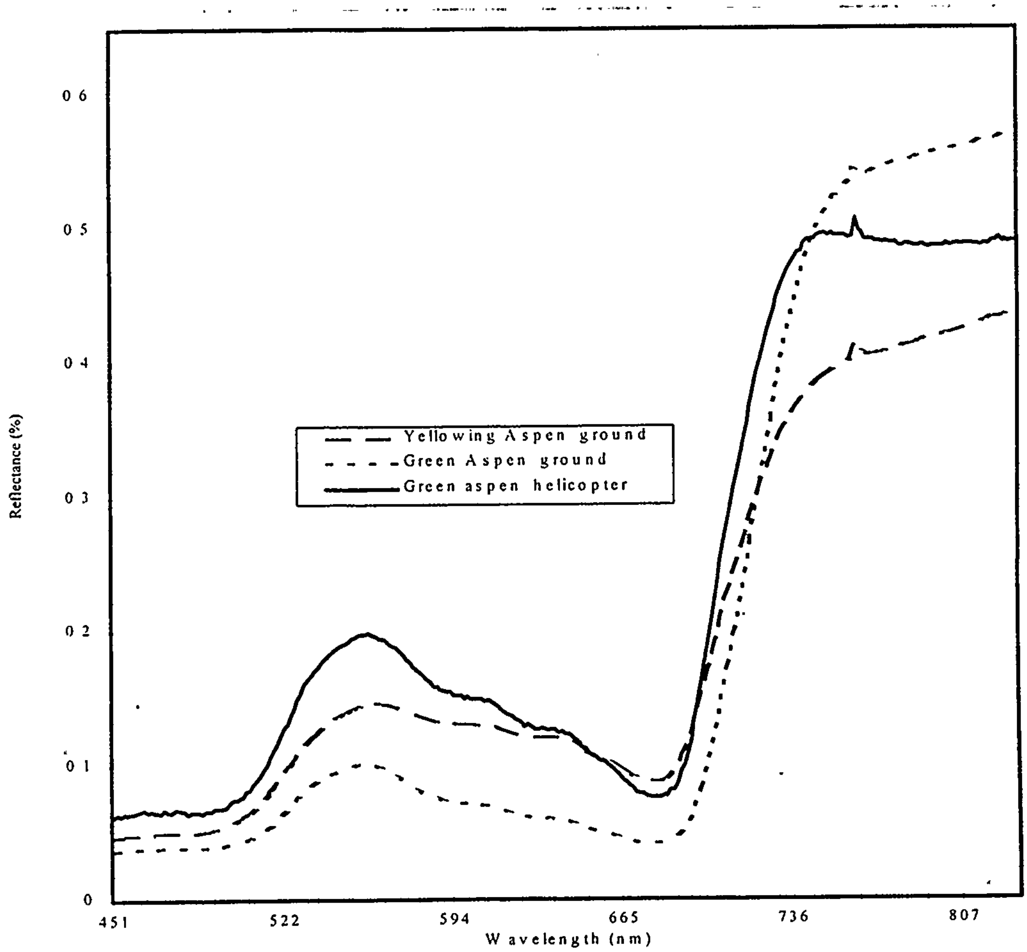

Figure 3.11: Aspen spectra from helicopter

Due to scheduling difficulties, the only time the helicopter was available was between 9:30 and 10:15 AM. This posed a serious problem due to the low sun angle which produced illumination conditions much different than those experienced during the *casi* flights. The only features which were fully illuminated were the sunward sides of tree crowns and large clearings. This was a major problem with the mature lodgepole pine and white spruce due to the structure of the tree crowns which resulted in small sunlit crowns surrounded by large areas of shadow which, when combined with the helicopter movement, prevented an accurate target lock when using the spectrometer.

3.4.3 Recommendations from the helicopter test

Detailed planning is essential for the success of any work done in a helicopter as there is no time available for creating tables or even for deciding on how many targets to sample. All activities must be fully planned and ready to go. Spectra should be taken from a viewing angle closely corresponding to that from which the imagery will be obtained and at the same time of day to ensure consistent illumination conditions. However, it must be accepted that it is practically impossible to accurately get the correct view angle. Another important issue is that maintaining the correct height of the sensor over the target is important for maintaining the desired spatial resolution. As a result, some method should be used for accurately determining the height of the helicopter above the target. This is very important as spatial resolution has been shown to have a significant impact on the spectra obtained (Ekstrand, 1994). Another difficulty with the helicopter was that the blade motion caused considerable motion in the canopy of the plants which almost certainly resulted in alterations in the spectral response.

The problems encountered during the flight certainly brought into question the validity of spectrometer readings obtained from helicopters which are used in other published studies. It is suggested that a preferable method for obtaining spectra over a canopy would be through the use of a crane or 'cherry picker'. This would provide a much more stable and controllable platform than a helicopter but would only be useful for studies in a small area. In spite of difficulties encountered, the flight was a good learning experience and provided useful information.

3.5 KANANASKIS *CASI* IMAGERY

The *casi* imagery of the Kananaskis study site was obtained on September 15, 1995 at a spatial resolution of 2.5 meters.

Table 3.1 shows the fifteen bands which were collected. The wavelength values shown are the wavelengths of the centre of each channel and the +/- values indicate the bandwidth of each channel.

casi channel	Wavelength (nm)
1	449.4nm+/- 11.2nm
2	487.4nm+/- 10.4nm
3	520.2nm+/- 5.9nm
4	534.4nm+/- 5.9nm
5	548.6nm+/- 5.9nm
6	585.1nm+/- 8.6nm
7	629.8nm+/- 8.7nm
8	674.6nm+/- 8.7nm
9	702.5nm+/- 4.2nm
10	709.7nm+/- 4.2nm
11	743.1nm+/- 5.1nm
12	752.1nm+/- 5.1nm
13	772.0nm+/- 5.1nm
14	781.0nm+/- 5.1nm
15	803.7nm+/- 6.0nm

Table 3.1: Kananaskis *casi* channels

The Kananaskis imagery was obtained by ITRES Research Ltd. for the purposes of testing a new *casi* instrument. ITRES personnel agreed on short notice to acquire the imagery over the Kananaskis study area and provided it free of charge. While the bands were selected by ITRES personnel for their general application to forestry studies, the imagery does provide a good sampling across the visible and near-infrared wavelengths in all areas indicated by the field spectrometer tests and should therefore be appropriate for use in this study. An image of the Kananaskis study area is shown in Figure 3.2.

3.6 Image pre-processing

Raw *casi* imagery contains radiometric and geometric distortions which should be corrected prior to analysis of the data. In the following Section, the processes which were applied to the Kananaskis imagery will be discussed.

3.6.1 Radiometric correction

Radiometric correction of the Kananaskis imagery was performed by ITRES Research Ltd. personnel. Additional processing was undertaken to convert this image set into a reflectance image using a pseudo-invariant feature as outlined in a paper by Freemantle, et al (1992). The radiance values produced by the radiometric correction process are affected by a variety of factors including the sensor configuration, variations in scene illumination, and atmospheric conditions. The resultant radiance values, however, are not unique signatures of objects being viewed. In order to allow for comparisons of imagery obtained on different days or with different sensors, it is necessary to convert the radiances into reflectance values. The use of reflectance images is necessary for a number of operations including change detection which requires accurate, comparable target reflectance values. Spectra or training signatures obtained from reflectance images are then transferable to other reflectance images which greatly increases the potential applications and value of remote sensing.

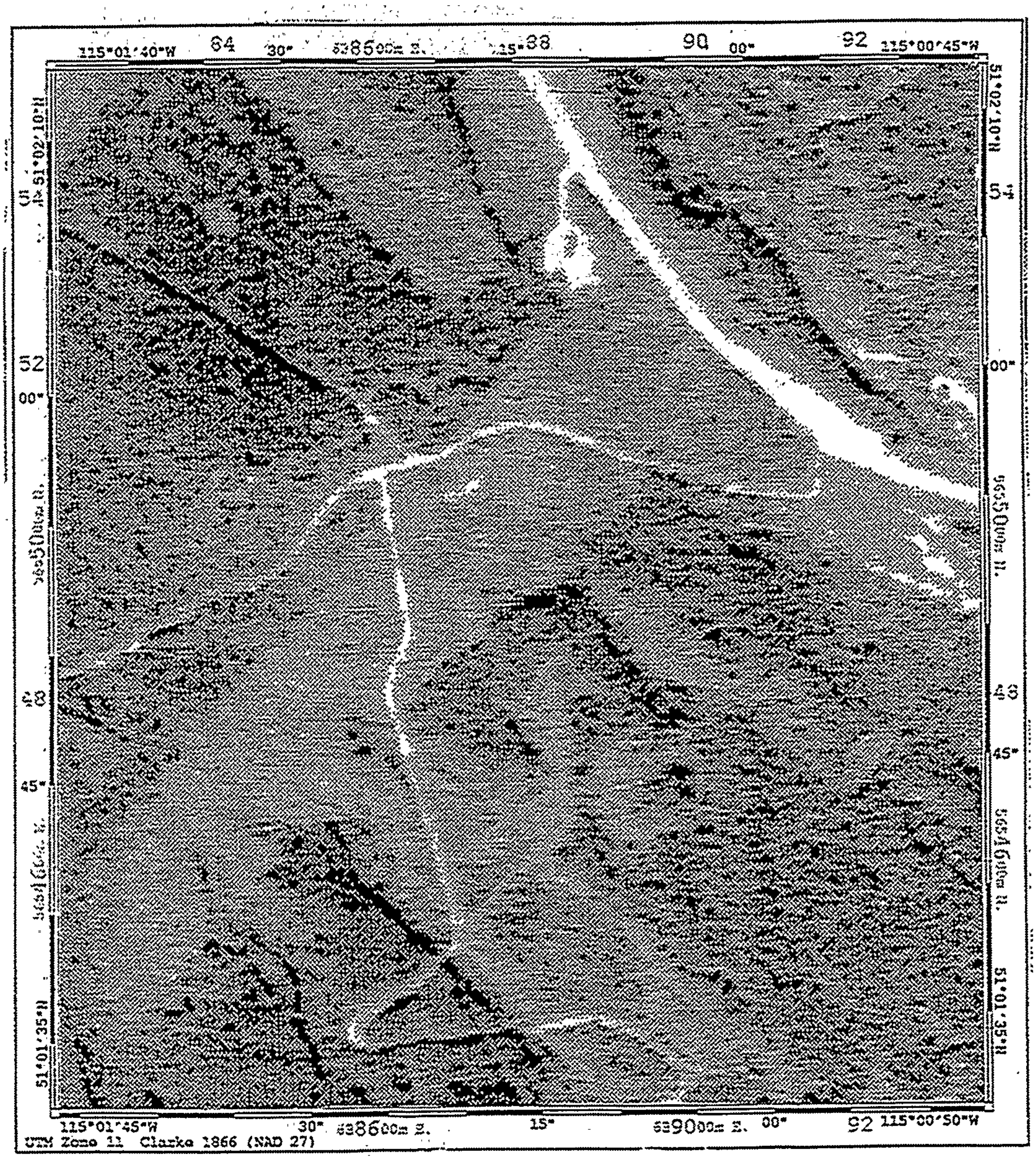

Figure 3.12: Kananaskis study area

In order to convert the radiance image into a reflectance image, a calibration process was performed by obtaining the spectral reflectance of a pseudo-invariant object and normalizing the radiance image based on the reflectance value of the pseudo-invariant object. A pseudo-invariant feature is an object which has the following characteristics (Freemantle, et al, 1992):

1. slowly varying spectral reflectance;
2. approximately Lambertian reflectance for typical viewing geometries;
3. seasonal invariance of reflectance for typical remote sensing observing conditions.

Objects which have been found to have these properties include gravel pits, roof tops, parking lots and roads. A wide gravel road which was prominent in the Kananaskis imagery was used as a pseudo-invariant feature for the creation of a reflectance image.

Reflectance values for the road were obtained on September 16, 1995 using an ASD hand-held spectrometer. To improve the accuracy of the results, the reflectance of the road was obtained at approximately the same time of day and in the same atmospheric conditions as those reported during the *casi* acquisition. The first step in the creation of the reflectance image was to determine a calibration constant by using the expression (Freemantle, et al, 1992):

$$reflectance\_calibration\_constant = \frac{ASD\_reflectance}{casi\_DN} \tag{3.1}$$

Reflectance values for each *casi* channel were extracted from the ASD spectrometer data collected for the gravel road for use in Equation 1 and are shown in Table 3.2. The reflectances are also displayed graphically in Figure 3.13. *Casi* DN values for the gravel road were extracted from the *casi* by averaging a sample of pixels and are also shown in Table 3.2. Equation 1 was then used to calculate the calibration constants for each channel (Table 3.2). The calibration constants were then applied to each *casi* channel to calibrate the image to reflectance values using Equation 2 (Freemantle, et al, 1992).

$$reflectance = casi\_DN \bullet reflectance\_calibration\_constant \quad (3.2)$$

Channel	Reflectance	*Casi* DN values	Calibration constant (ζ)
1	0.14991	4340	0.000035
2	0.15706	5566	0.000028
3	0.17013	5853	0.000029
4	0.17518	6363	0.000028
5	0.18152	6494	0.000028
6	0.19166	6548	0.000029
7	0.19811	6000	0.000033
8	0.20459	6020	0.000034
9	0.20895	5849	0.000036
10	0.20968	6040	0.000035
11	0.21398	5888	0.000036
12	0.21544	5905	0.000036
13	0.21783	5582	0.000039
14	0.21834	5625	0.000039
15	0.22107	5174	0.000043

Table 3.2: Gravel road reflectances, *casi* DN's, and calibration coefficients

The use of only one pseudo-invariant object to generate the calibration constant (ζ) means that the effect of atmospheric and background radiances is not accounted for (Freemantle, et al, 1992). The effect of this would be to cause a reduction in the value of the reflectance values which are produced from this process. However, the magnitude of this error is dependent on the flying height of the sensor and at the altitude that the *casi* imagery was flown this error should be quite small (Freemantle, et al, 1992).

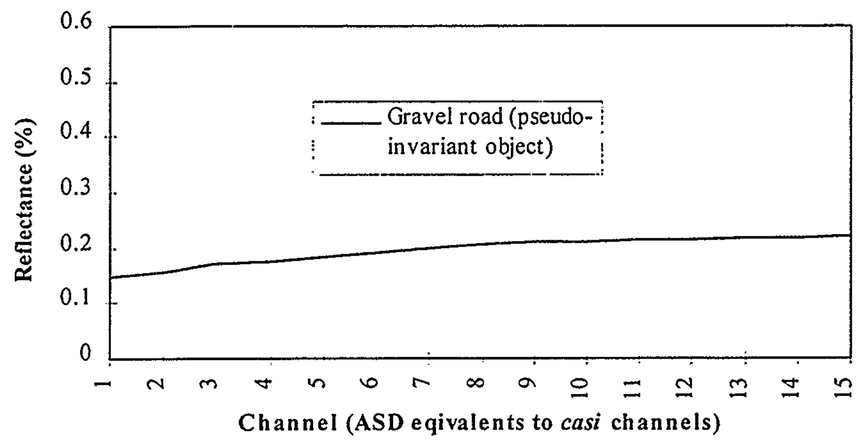

Figure 3.13: Gravel road reflectance from ASD spectrometer

3.6.2 Geometric Correction

Due to a number of factors, a detailed geocorrection was not applied to the Kananaskis imagery. It is understood that considerable position errors are present in the imagery. However, it was felt that the lack of accurate geocorrection would not significantly impact the results of this study. Training areas were derived from a combination of ground-truth sketches and photos of the site. This was possible because the areas which were trained for the classifier and for accuracy assessment were homogenous groupings of each class and were easily located on the image.

The geocorrection of *casi* imagery has been discussed and illustrated by a number of researchers, and while this study did not require accurate geocorrection, it should be noted that any data being integrated into a geographical information system (GIS) or decision support system (DSS) should undergo a rigorous geocorrection process. Further details of the geocorrection process can be found in Cosandier, et al (1992).

3.7 GROUND MEASUREMENTS

Extensive ground truthing was undertaken in August and September 1995 in order to accurately characterize the site in preparation for analysis of the *casi* imagery. Detailed sketch maps were developed and a large number of photographs were taken to assist in the classification process.

3.8 DEVELOPMENT OF TRAINING AND TESTING AREAS

Training and testing areas for the Kananaskis study site were developed using a combination of sketch maps created during ground truthing, photographs of the site, and Alberta Forestry Forest Inventory Maps. The training areas were required to prepare class signatures for input into the maximum likelihood classifier (MLC) for the purposes of classifying the imagery into several landcover classes, while the testing areas were required for an appraisal of the accuracy of the classification derived from the testing areas.

The selection of training and testing areas was generally straight forward due to the high separation of species in the area. However, as discussed in Chapter 4, high resolution imagery, such as the 2.5 meter resolution *casi* imagery used in this study, can cause problems when using the MLC due to the presence of both sunlit and shaded trees which tend to make class signatures skewed or even bimodal (Gougeon, 1993). One of the underlying assumptions of the MLC is that class distributions are normally distributed (PCI, 1994). If this is not the case then the MLC cannot accurately classify an image.

Even if the signatures are not bimodal, signatures can end up having very wide ranges with considerable overlap between different classes which results in a large number of unclassified pixels. A shadow class was included in this classification in an attempt to reduce some of the classifier confusion caused by shadowed areas. The "shadow" class, in essence, acts as a filter to eliminate pixels which would otherwise cause wide or bimodal class distributions which would confuse the MLC. It is understood that areas classed as shadow will in fact belong to one of the other classes. However, given the limitations of the MLC it was felt that this was a reasonable approach to improve the accuracy of the classifier when using high resolution imagery.

Since the position of shadow areas cannot be accurately located using ground truthing, a process had to be adopted for selecting 'shadow' training pixels. The process adopted involved the selection of pixels of very low spectral response on the shaded side of pixels with high spectral response. An attempt was made to use large areas of shadow which were easy to identify such as an area which existed along the base of a hill which was oriented away from the sun. In addition, during the defining of training areas for all other classes, pixels of low reflectance values were not included in training classes for the individual classes. In essence, the approach could be considered a "lit side" classification scheme in which training pixels are only derived from the sunlit portions of the trees. Gougeon (1994) compared several different classification techniques for high-resolution MEIS images and found that an approach which used pixels from the lit side of tree crowns had the highest inter-species classification accuracy. The process also mimicked the operation of tree isolation algorithms which have been suggested by several researchers as a method of improving the classification of high-resolution imagery. Tree isolation algorithms are still under development by other researchers and were not available for this study.

The classification scheme outlined on the following page was developed based on experience from the ground truthing and from an examination of the imagery. Testing and training areas were delineated for each class.

1. aspen
2. grass
3. gravel
4. mature lodgepole pine
5. mistletoe-infested mature lodgepole pine
6. pavement
7. shadow
8. shrubs/understory
9. spruce
10. young lodgepole pine

3.9 IMAGE ENHANCEMENT

Many image enhancement techniques involving band combinations, band ratios, or band transformations have been developed to either highlight features of interest which are not evident in the raw imagery, or to reduce the number of channels of data (image dimensionality) while preserving the information of importance. When using multispectral or hyperspectral imagery it is necessary to reduce the dimensionality of the data set in order to be able to properly analyze the data using the MLC. In the following Section, the image enhancement techniques which were used during this project will be discussed. A list of all the resultant channels can be seen in Table 4.3. The value of the image enhancements which are produced in this Section to the goal of discriminating between healthy and dwarf mistletoe-infested lodgepole pine will be determined in Chapter 4 during the channel selection process.

3.9.1 Shadow reduction through image normalizing

Shadows are a very serious problem when dealing with high or mid-resolution imagery. One method used to reduce the effect of illumination changes due to shadowing involved a normalizing procedure whereby the reflectance of each individual pixel was divided by the total reflectance in all spectral bands for the pixel (Gong, 1993). The process of division acts to negate extraneous multiplicative factors that act equally on the channels being divided and thus objects of the same class should then appear similar regardless of the illumination conditions. Thus the use of normalized channels should provide a superior classification result than the original channels. This process was applied to the *casi* image and the resultant channels were examined during the channel selection process.

3.9.2 Principal component analysis

Principal component analysis (PCA) is a process by which the information content of a large number of image channels is compacted into a small number of channels by factoring the total variation in the data into mutually orthogonal components (Jensen, 1986). While the number of channels is reduced, the total variation in the data is preserved which makes this approach very attractive as a method for reducing the number of channels to be analysed. As mentioned above, reducing the dimensionality of a data set is very important when using imagery with a large number of channels.

The first few significant principal components can then be used during image analysis as they contain the vast majority of the information in the imagery. While the first principal component typically contains about 80% of the total variance in the data, it has been found that the information of importance for some applications can be found in the smaller components such as the 4th or 5th principal components which are often considered insignificant due to the fact that they represent a very small portion of the variability in the data set. Further details on the theory of principal component analysis can be found in many texts including Hord (1986) and will not be discussed further in this paper.

Principal component	Eigenvalue	Deviation	%Variance
1	0.1156140E+08	0.3400206E+04	83.03%
2	0.2124689E+07	0.1457631E+04	15.26%
3	0.1512684E+06	0.3889324E+03	1.09%
4	0.4962052E+05	0.2227566E+03	0.36%
5	0.2046256E+05	0.1430474E+03	0.15%

Table 3.3: First 5 principal components of the Kananaskis image

The first 5 principal components of the Kananaskis *casi* imagery were calculated and are shown in Table 3.3. The corresponding eigenvectors are shown graphically in Figure 3.14. While a brief analysis of each principal component is provided below, it should be noted that a detailed examination of the principal components could form the basis for an entire study and was beyond the scope of this project. The principal components will be analysed during the channel selection process to determine their application to this project. The eigenvectors for PC1 show positive contributions from all spectral bands and an image of PC1 showed detail in all regions of the image. This is to be expected as PC1 contained over 83% of the variation in the imagery and thus shows the major features in the image. The eigenvectors for PC2 indicate that it formed by a contrast between reflectance in the NIR and visible wavelengths. As a result, PC2 could be expected to distinguish between vegetated and non-vegetated areas or between different species. A study by Blackburn and Milton (1994) with similar *casi* imagery found that PC2 provided differentiation between deciduous and coniferous trees.

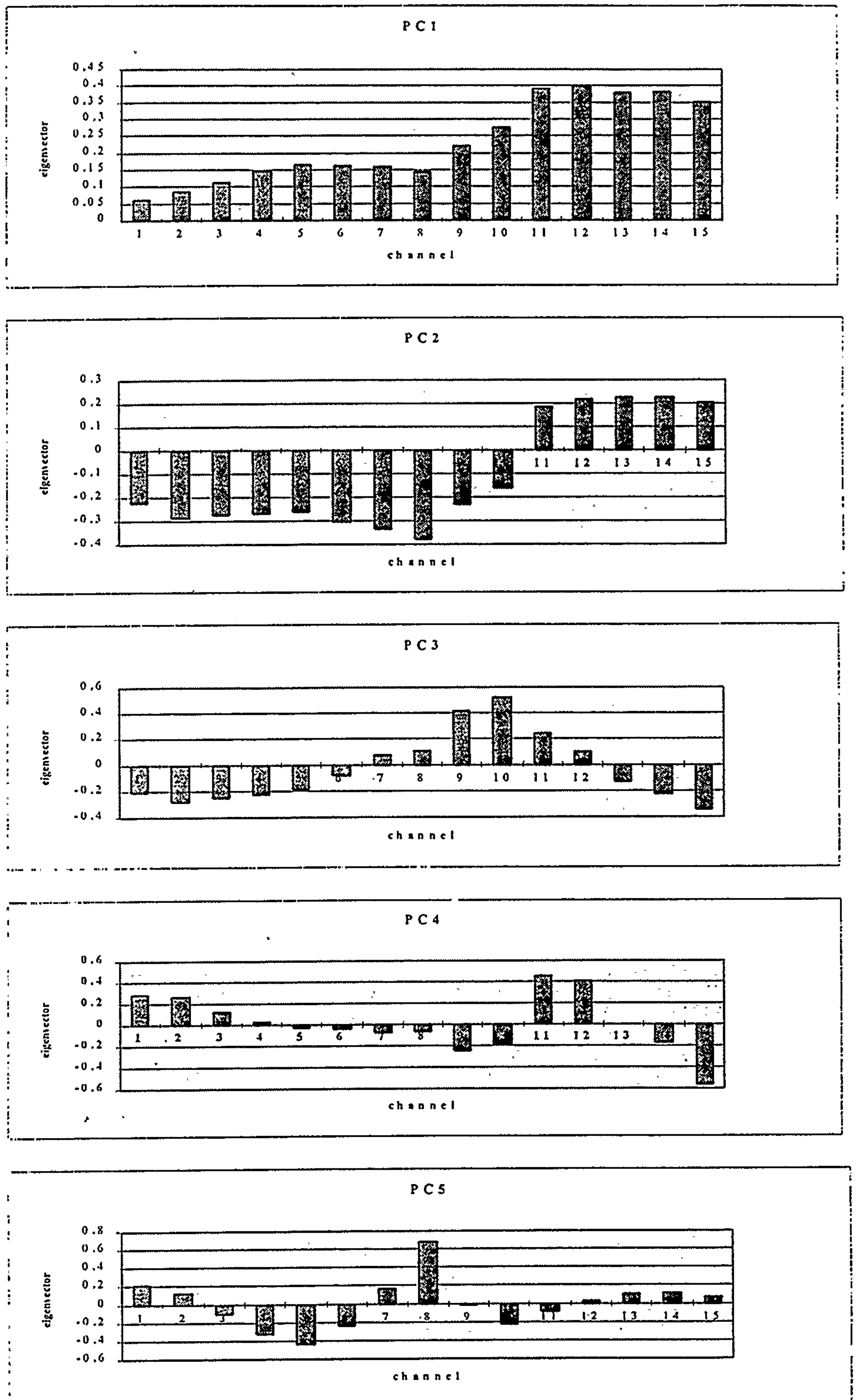

Figure 3.14: Eigenvectors for PC1 to PC5

PC3 is somewhat confusing in that it contained a contrast between a positive contribution from channels on the red edge and negative contributions from both blue and green channels and most of the NIR channels. Analysis of a PC3 image did not reveal any conclusive information on the content of the image. Blackburn and Milton (1994) found that PC3 was related to the "openness" of the canopy.

The eigenvector loadings of PC4 present a confusing picture with both a positive and a negative influence from the NIR channels. This was combined with a contrast between blue channels and channels on the red edge. An image of PC4 did not reveal any useful data and it was not possible to determine anything of value from this component.

The main components of PC5 were a contrast between a positive contribution from red channels and a negative contribution from green channels. Thus, it might be possible that PC5 would provide information on vegetation health or species separation.

3.9.3 RVI

A ratio which is similar to the RVI common to TM imagery been used to by several researcher, including O'Connor, et al (1995), to highlight changes in vegetation health using mid and high resolution *casi* imagery. In general, unhealthy vegetation has been found to have a decrease in NIR reflectance and an increase in red reflectance which would result in a significantly lower RVI than with healthy vegetation. The process of division also acts to remove the effects of factors such as topography or sun angle which act equally on all channels so that one type of object will appear the same regardless of differences in topography or sun angle (Hord, 1986).

The RVI for this project was calculated by the following:

$$RVI = \frac{ch\_11}{ch\_8}; \qquad (3.3.)$$

where channels 8 and 11 had the following wavelengths:

- Channel 8: 674.6nm (red)
- Channel 11: 743.1nm (NIR)

In the case of dwarf mistletoe-infested lodgepole pine, while the red reflectance was seen to increase in the field spectrometer tests, NIR reflectance was also increased which is the opposite of what was expected when the RVI was developed. Therefore, based on the field spectrometer tests, in the case of lodgepole pine with dwarf mistletoe, there would actually be a small increase in the NDVI. Based on the field spectrometer tests, the NDVI may not be a good indicator of dwarf mistletoe, but it will be included in the study due to its wide acceptance as an indicator of vegetation health.

3.9.4 NDVI

A ratio which is similar to the normalized difference vegetation index (NDVI) common to TM imagery has been used to highlight changes in green biomass, chlorophyll content, and moisture content by other researchers using mid and high resolution *casi* imagery for forestry applications including O'Connor, et al (1995). In general, unhealthy vegetation has been found to have a decrease in NIR reflectance and an increase in red reflectance which would result in a lower NDVI than with healthy vegetation.

For this project the NDVI was calculated by the following:

$$NDVI = \frac{ch\_11 - ch\_8}{ch\_11 + ch\_8}; \qquad (3.4.)$$

where channels 8 and 11 had the following wavelengths:

- Channel 8: 674.6nm (red)

  Channel 11: 743.1nm (NIR)

In the case of dwarf mistletoe-infested lodgepole pine, while the red reflectance was seen to increase in the field spectrometer tests, NIR reflectance was also found to increase which is the opposite of what was expected when the NDVI was developed. Therefore, based on the field spectrometer tests, in the case of lodgepole pine with dwarf mistletoe, there would actually be a small increase in the NDVI. Based on the field spectrometer tests, the NDVI may not be a good indicator of dwarf mistletoe, but it will be included in the study due to its wide acceptance as an indicator of vegetation health.

3.9.5 Texture analysis

Texture is an extremely important characteristic of natural objects for image analysis and classification. Spectral features only contain information about the average tonal variation in the bands of an image. No information is provided about the context of the pixel. Textural features contain information about the spatial distribution of tonal variations within a band (PCI, 1992) which means that the information from neighbouring pixels is considered to provide contextual information. Many researchers have concluded that humans use much more information than the basic spectral information when viewing a scene including texture, pattern recognition, and context. Studies by several researchers, including Ekstrand (1994), have indicated that at a spatial resolution of 0-5 meters, texture is often as important as spectral information.

The texture of a lodgepole pine forest varies with age and health. Young pine stands (less than 5 years old) have a course texture due to the large amount of understory visible between the young pines. As the stand age increases, texture decreases to due canopy closure. A healthy mature stand of pine should have the finest texture with texture becoming more coarse in old-age stands due to dying crowns and tree mortality. In contrast, a mature stand of lodgepole pine with serious dwarf mistletoe infestation would have a much more coarse texture than a comparably aged healthy stand due to the presence of dead and dying limbs and crowns. In addition, stands of spruce also have different texture as is evident when viewing aerial photographs. Given that spectral differences may be quite small between healthy and unhealthy lodgepole pine, it is very important to include a measure of texture in any analysis of mistletoe using *casi*. As a result, several measures of texture were calculated and analyzed as input into the classification process along with the spectral information.

The texture measure used in this project is based on statistics derived from the co-occurrence matrix. Co-occurrence matrices calculate the relationship between a given pixel and a specified neighbour (PCI, 1992). Further details on co-occurrence-based texture measures can be found in many papers including Wang and He (1990).

Several measurements of texture were calculated and stored as new image layers which were used as additional channels during the channel selection procedure (i.e. each pixel has a grey-level value representing texture). The specific texture measure used was the Homogeneity texture filter contained in the TEXTURE analysis component of the Radar analysis package in the PCI EASI/PACE remote sensing analysis package. When it comes to choosing a texture algorithm little agreement is found among researchers. All studies using texture expressed the concern that it is very difficult to explain exactly what is actually being measured by a specific texture measure, and that the best measure can only be derived through trial and error. A future study could be made into deriving the best measure of texture for dwarf mistletoe applications.

A texture algorithm passes a filter consecutively over all pixels in the image and determines the level of texture within the filter and the resultant value is placed in the centre pixel of the filter area. The size of filter used is extremely important to ensure that the desired texture is being measured. If the filter is too large, small texture features will be missed and if the filter is too small, then larger features will be missed. The filter size was chosen based on an analysis of the average size of a lodgepole pine crown so that the texture measurement would indicate different levels of canopy closure. A filter size of 5 x 5 pixels was chosen based on the assumption that an individual tree crown is approximately 2 to 3 pixels in size. A healthy stand of lodgepole pine should have a closed crown and therefore would have a finer texture using this filter size than an unhealthy stand with lower crown closure.

Three texture measures were calculated for this project. The first texture measure involved the application of the texture algorithm on the first principal component image channel. Since the texture algorithm can only be applied to a single channel of imagery, the first principal component image (PC1) was used because it contained 83 % of the total variation in the data.

The second texture measure was derived by applying a Laplacian edge detector filter to the PC1 and then applying the homogeneity texture algorithm. Since the purpose of using a texture measure is to include some measure of the local variations in brightness values, an edge detector filter was first applied to the PC1 to highlight these changes and then the homogeneity texture algorithm was applied to the edge-enhanced image.

The third texture measure was simply the results of the Laplacian edge detector filter applied to PC1. This method was used based on the assumption that the edge detection image itself could provide enough information on the texture of the image to improve the classification. Texture algorithms are very computationally-intensive and require a significant amount of time to process a large image while the edge detector requires much less processing time.

4. KANANASKIS IMAGE CLASSIFICATION

In this chapter, the classification procedure undertaken on the Kananaskis imagery will be discussed. In Section 4.1, an optimization procedure will be discussed which was developed to select the optimal set of bands, band combinations, band ratios, or band transformations to best discriminate between the healthy and dwarf mistletoe-infested lodgepole pine. The imagery was then classified using the maximum likelihood classifier (MLC) as discussed in Section 4.2. Results of the classification procedure are presented and discussed in Section 4.3.

4.1 IMAGE DIMENSION REDUCTION

With multispectral and hyperspectral imagery, a vast amount of information is available for analysis. In most cases, the majority of the data is not useful for the task being performed. In addition, it has been found that when using the maximum likelihood classifier (MLC), classification accuracy does not increase and, in fact, often decreases if more than an optimal number of channels are used. Reinartz (1993) recommended using 5 or 6 channels for forest damage classification and others have recommended 6 channels for classification using the MLC (PCI, 1994). It is, therefore, essential to determine what information is actually important in order to ensure that the correct information is being input into the classifier.

As was discussed in Chapter 3, a number of band combinations, band ratios, and band transformations can be developed which produces additional channels for analysis. Most band transformations or combinations are intended to highlight features of interest or to concentrate important information into a smaller set of channels, and thus serve to reduce the dimensionality of the data. However, during initial research, the use of such indices increases the number of channels which must be analyzed to determine their usefulness to the task being performed.

The image dimensionality reduction technique used in this project involved a three-step process. Stage one involved the calculation of the band combinations, band transformations and band ratios which were discussed in Chapter 3. Stage two involved the use of correlation analysis and information from the field spectrometer tests to reduce the number of original *casi* bands. Stage three involved the analysis of the remaining image channels and image enhancements using a channel selection algorithm which employed an analysis of the class signatures in order to select the best set of channels to discriminate between the healthy and dwarf mistletoe-infested mature lodgepole pine.

4.1.1 Initial channel reduction: correlation analysis

The correlation matrix was used as to reduce the dimensionality of the original 15 channel *casi* data set. The correlation matrix calculates to what extent two channels are correlated. A correlation of 1 indicates a perfect positive correlation, a value of 0 indicates no correlation, and a value of -1 indicates a perfect negative correlation (Jensen, 1986).

The correlation matrix for the Kananaskis *casi* channels is shown in Table 4.1. Analysis of the correlation matrix indicated a high correlation between channels 1 through 10 (visible) and a very high correlation between channels 11 through 15 (NIR). The lowest correlations were found between the blue channels (channels 1 & 2) and the near-infrared channels (channels 11-15).

It is important to keep in mind when utilizing a correlation matrix for image dimension reduction that the correlation matrix only indicates the interdependence of two channels and does not provide any information directly relating to the usefulness of each channel in discriminating an object of interest. It is, therefore, important to also consider other information when deciding on which channels to keep. This is especially important when, as in this project, a large group of highly correlated channels exists. The information provided by the spectra obtained using the field spectrometer (Chapter 3) was used in conjunction with the correlation matrix for reducing the number of *casi* channels.

	1	2	3	4	5	6	7	8	9	10	11	12	13	14	15
1	1														
2	0.98	1													
3	0.96	0.98	1												
4	0.91	0.94	0.98	1											
5	0.88	0.91	0.98	0.98	1										
6	0.90	0.93	0.98	0.98	0.98	1									
7	0.90	0.93	0.97	0.97	0.98	0.98	1								
8	0.92	0.94	0.96	0.94	0.93	0.96	0.98	1							
9	0.73	0.76	0.86	0.91	0.93	0.93	0.94	0.88	1						
10	0.63	0.66	0.78	0.86	0.89	0.87	0.87	0.80	0.98	1					
11	0.34	0.37	0.52	0.63	0.68	0.63	0.59	0.49	0.8	0.89	1				
12	0.32	0.35	0.50	0.61	0.67	0.61	0.57	0.47	0.77	0.87	0.98	1			
13	0.31	0.34	0.50	0.60	0.66	0.60	0.55	0.45	0.76	0.85	0.98	0.98	1		
14	0.31	0.35	0.50	0.61	0.66	0.60	0.55	0.45	0.75	0.84	0.98	0.98	0.98	1	
15	0.31	0.35	0.50	0.61	0.65	0.60	0.54	0.45	0.75	0.83	0.97	0.98	0.98	0.98	1

Table 4.1: Correlation matrix - *casi* channels 1 to 15

No especially distinguishing spikes or radical differences were found at any particular wavelength during the field spectrometer tests which indicated that a single defining band did not exist and that a combination of information from different wavelengths would be required. Based on the analysis of the field spectrometer results, band selection for a classification intended to differentiate between healthy and dwarf mistletoe-infested lodgepole pine should emphasize the NIR wavelengths (750-850nm) and the peak of green reflectance (~550nm). Additional channels should be selected from the area of the spectrum between the upper portion of the green wavelengths and the middle portion of the red wavelengths (550-650nm) as well as the lower portion of the green wavelengths (500-550nm), both regions in which small differences were evident in the field spectra of lodgepole pine.

Since *casi* channels 1 to 10 were highly correlated, a decision had to be made on which channels were best retained. Channel 1 was rejected because of it is at the low end of the blue portion of the spectrum which is severely affected by view angle effects which are prevalent in airborne imagery because of the low elevation of acquisition. Channel 2 would be less affected by view angle effects and was selected to preserve some of the information from the blue wavelengths as this portion of the spectrum was identified during field spectrometer tests as being of some potential. Channel 5 is at the green peak of reflectance which was identified during the field spectrometer tests as potentially being very important for dwarf mistletoe identification. Channel 8 is at the low point of the red chlorophyll absorption well which is of importance for vegetation analysis due to the absorptive characteristics of chlorophyll in healthy plants at these wavelengths. Channel 10 is positioned on what researchers have termed the red edge which is the transition from the red absorption well to the near infrared plateau which has been found by some researchers to be sensitive to variations in plant health and was identified during helicopter spectrometer tests as an area of potential importance. Channels 12 and 13 are both positioned on the near infrared plateau of vegetation which was identified during the field spectrometer tests as potentially being the most important region for the discrimination of healthy and dwarf mistletoe-infested lodgepole pine.

The resultant subset of the original *casi* channels which was selected was composed of *casi* channels 2, 3, 4, 5, 6, 8, 10, 11, 12, and 13. The correlation matrix was only used to select this initial subset of the original *casi* channels. It was felt that the correlation matrix did not provide enough project-specific information to choose the best subset of the remaining input channels shown in Table 4.2, and that additional information would be required to accurately choose the best subset of the *casi* channels, channel combinations, channel transformations and channel ratios to best distinguish between the healthy and dwarf mistletoe-infested lodgepole pine. Therefore, as described in Section 4.1.2, the remaining *casi* channels and the normalized channels, texture measures, and vegetation indices were further analysed using a channel selection algorithm which utilised class training signatures in determining the set of input channels for a classification of healthy and dwarf mistletoe-infested lodgepole pine.

4.1.2 Channel selection algorithm

The next stage in the image dimension reduction process involved the use of a channel selection algorithm provided in the PCI EASI/PACE remote sensing image processing package. Channel selection algorithms have been designed to select the channels which provide the best discrimination between various classes by analysing signatures generated for each class from training areas. For this project, the minimum parities divergence criterion was used to choose the best channels for the MLC. The minimum parities divergence algorithm was designed to select the channels which show the greatest discrimination between the two classes which are most similar, which in the case of this project, was the healthy lodgepole pine class and the dwarf mistletoe-infested lodgepole pine class.

This algorithm was chosen because the major goal of this project was to discriminate between the healthy and dwarf mistletoe-infested lodgepole. Other channel selection algorithms are available which are designed to optimize other parameters such as the average separation between all classes. It is quite possible that channels selected by another channel selection algorithm would have resulted in a greater accuracy of classification between the major species classes in the study area. However, the goal of this project was to discriminate between the two states of lodgepole pine, and this concept was not investigated further.

The 29 channels which were evaluated using the minimum parities divergence algorithm are shown in Table 4.2. The configuration of the channel selection algorithm in EASI/PACE limited the number of channels which could be analysed at one time which meant that a multi-step process had to be used to select the best 6 channels from the 29 input channels. As a result, the 29 channels were analyzed in separate groups with class signatures generated with each subset of channels for input into the channel selection algorithm. Additional selection steps were run to find the best 6 channels of the initial 29 channels which would best distinguish between the healthy lodgepole pine and the dwarf mistletoe-infested lodgepole pine. The 6 optimal channels which were selected are shown in Table 4.3. These channels were used as input into the classification process as discussed in Section 4.2.

In addition, a subset of the best 6 channels from the original *casi* channels was also selected using the channel selection algorithm (Table 4.4). No image enhancements were included in the channel selection procedure for this channel subset. This subset of channels will be used to create a classification which will be analysed to determine if any improvement in classification accuracy was provided by using the image enhancements which were included in the channel selection procedure for the 6 optimal channels.

Database channel number	Channel content description
1[1]	casi ch 2: 487.4 +/- 10.4nm
2[1]	casi ch 3: 520.2nm+/- 5.9nm
3[1]	casi ch 4: 534.4nm+/- 5.9nm
4[1]	casi ch 5: 548.6nm +/- 5.9nm
5[1]	casi ch 6: 585.1nm +/- 8.6nm
6[1]	casi ch 8: 674.6nm +/- 8.7nm
7[1]	casi ch 10: 709.7nm +/- 4.2nm
8[1]	casi ch 11: 743.1nm +/- 5.1nm
9[1]	casi ch 12: 752.1nm +/- 5.1nm
10[1]	casi ch 13: 772.0nm +/- 5.1nm
11[1]	Principal component 1 (PC1)
12[1]	Principal component 2 (PC2)
13[1]	Principal component 3 (PC3)
14[1]	Principal component 4 (PC4)
15[1]	Principal component 5 (PC5)
16[1]	texture: homogeneity on Laplacian Edge Detector of PC1
17[1]	NDVI (ch 8 & 11)
18[1]	RVI (ch 8 & 11)
19[1]	texture: homogeneity on PC1
20[1]	texture: Sobel Edge Detector on PC1
21[1]	Normalized casi ch 2
22[1]	Normalized casi ch 5
23[1]	Normalized casi ch 6
24[1]	Normalized casi ch 8
25[1]	Normalized casi ch 9
26[1]	Normalized casi ch 10
27[1]	Normalized casi ch 11
28[1]	Normalized casi ch 12
29[1]	Normalized casi ch 13

Table 4.2: Channels evaluated using channel selection algorithm

4.1.3 Discussion of optimal channel selection results

The 6 optimal channels which were selected as the best input into the MLC for the purpose of discriminating between healthy and dwarf mistletoe-infested mature lodgepole pine are shown in Table 4.3 and discussed in the following Section. The 6 optimal channels included database channels 2^1, 4^1, 13^1, 19^1, 21^1, 22^1 which correspond to *casi* channels centered at 520.2nm and 548.6nm, the third principal component, a texture measure, and two normalized channels centered on 487.4nm and 548.6nm respectively.

Channel 2^1 was *casi* channel 3 which, at 520.2nm, is at the low end of the green portion of the spectrum and is near the transition point between the chlorophyll absorption well of the blue wavelengths and the green reflectance peak. As such, changes in the health of the lodgepole pine, particularly changes in chlorophyll concentrations would affect this portion of the spectra.

Channel 4^1 was *casi* channel 5 which at 548.6nm lies at the peak of the green reflectance peak of vegetation. Decreases in plant health cause changes in the level of green reflectance due to variations in chlorophyll levels as was observed during field spectrometer tests.

Channel 13^1 was the 3rd principal component (PC3). Blackburn and Milton (1994) performed an in-depth study on the principal components using a similar *casi* data set and found that PC3 contained information relating to the "openness" of the canopy (texture). If this is the case, then the variations in texture which exist between the canopies of healthy and dwarf mistletoe-infested lodgepole pine would explain the selection of PC3.

Channel 19^1 was a texture measure derived from the 1st principal component (PC1). The selection of a texture channel is in agreement with the findings of other researchers who found that texture is very important when classifying mid and high resolution imagery.

Best 6 channels from original *casi* channels	
Database channel	**Channel content**
2^1	520.2nm
4^1	548.6nm
6^1	674.6nm
8^1	743.1nm
9^1	752.1nm
10^1	772.0nm
Optimal 6 channels from all input channels	
Database channel	**Channel content**
2^1	520.2nm
4^1	548.6nm
13^1	Principal component 3 (PC3)
19^1	Texture
21^1	Normalized 487.4nm
22^1	Normalized 548.6nm

Table 4.3: Channel selection results

Channel 21^1 is the normalized version of *casi* channel 2 which, at 487.4nm, lies at the upper end of the blue portion of the spectrum. Channel 22^1 is the normalized version of *casi* channel 5, which was also selected by the channel selection algorithm.

The 6 optimal channels which were selected should provide the highest level of discrimination between healthy and dwarf mistletoe-infested lodgepole pine possible with this data set and will be used for 2 classifications which are explained in Section 4.2.1.

4.1.4 Discussion of *casi* channel selection results

In the following Section the best 6 *casi* channels which were selected from the original *casi* channels are discussed. The channels selected were database channels 2^1, 4^1, 6^1, 8^1, 9^1, 10^1 (Table 4.4) which correspond to *casi* channels centered at 520.2nm, 548.6nm, 674.6nm, 743.1nm, 752.1nm, and 772.0nm.

Channel 2^1 was *casi* channel 3 which, at 520.2nm, is at the low end of the green portion of the spectrum and is near the transition point between the chlorophyll absorption well of the blue wavelengths and the green reflectance peak. As such, changes in the health of the lodgepole pine, particularly changes in chlorophyll concentrations would affect this portion of the spectra.

Channel 4^1 was *casi* channel 5 which at 548.6nm lies at the peak of the green reflectance peak of vegetation. Decreases in plant health cause changes in the level of green reflectance due to variations in chlorophyll levels.

Channel 6^1 was *casi* channel 8 which at 674.6nm is at the low point of the red well of chlorophyll absorption which is impacted by changes in health of plants which cause corresponding changes in plant health. Field spectrometer tests indicated that reflectance increases in this portion of the spectrum for infested lodgepole pine.

Channel 8^1 was *casi* channel 11 which at 743.1nm lies on the NIR plateau. The spectrum of lodgepole pine was shown in the field tests to undergo large changes in this portion of the spectrum. Channel 9^1 at 752.1nm, and channel 10^1 at 772.0nm are also located on the NIR plateau.

This subset of *casi* channels was used to create a classification (Section 4.2.1) which was then compared to a classification created from the 6 optimal channels to determine if any improvement in classification accuracy of dwarf mistletoe was provided by the addition of the image enhancements during the channel selection process for the optimal 6 channels.

4.2 MAXIMUM LIKELIHOOD CLASSIFIER

The maximum likelihood classifier (MLC) was used to classify the *casi* imagery from the Kananaskis study area. The MLC was designed for use with low resolution satellite imagers such as the Thematic Mapper (TM) or SPOT and is a pixel-based classifier which compares the value of each pixel to the values of classes which are selected during a training process utilizing apriori knowledge of the area being classified or of the classes being used. The MLC evaluates both the variance and correlation of the training signatures of the different classes when assigning each pixel to a class. Each pixel is then placed into the class to which it has the highest likelihood of belonging.

When used for classifying mid-resolution imagery such as the 2.5 meter *casi* used in this study, the MLC is limited by its design. One of the underlying assumptions of the MLC is that class distributions are normally distributed (PCI, 1994). As will be discussed later in this Section, the nature of mid-resolution imagery is such that this assumption is not always true. In addition, since the MLC is a pixel-based classifier, it does not take into account the context of each pixel. It has been found by many researchers that neighbourhood-based features such as texture are extremely important with mid-resolution imagery. This shortcoming of the MLC can be partially remedied by including a measure of texture into the classification process which will provide neighbourhood information. Texture measures were discussed in Section 3.9.5

As discussed in Section 4.1, it has be shown that the accuracy of the maximum likelihood classifier often decreases with an increase in the number of input bands past an optimal number. The optimal number of input channels has been shown by many researchers to be 6 channels (PCI, 1994). As a result, if, as in this project, more than six channels of data are available for analysis it is necessary to reduce the dimensionality of the data set to approximately six input channels. The process of image dimension reduction was discussed and implemented in Section 4.1.

4.2.1 Kananaskis classifications

Three MLC-derived classifications were performed on the Kananaskis *casi* imagery and are discussed in the following Sections.

4.2.1.1 Species-based classification

The first classification performed was a species-based classification intended to separate the major species in the study area (Figure 4.1). While the main object of this study was the discrimination of healthy and dwarf mistletoe-infested lodgepole pine, it was decided to use the opportunity to also conduct a brief study of the accuracy of species discrimination using the MLC with the *casi* data. This classification was carried out to determine how accurately the major species in the study area could be classified using the 6 optimal channels which were selected during the image dimension reduction process (520.0nm, 548.6nm, PC3, Texture, normalized 487.4nm, normalized 548.6nm - see Table 4.3). The results of this species-based classification are shown in Figure 4.1 and Table 4.4 and the accuracy of the classification is outlined and discussed in Section 4.3

Class	Code	Pixels	Hectares	% Image
pavement	1	663	.49	.34
gravel	2	1828	1.36	.94
white spruce	3	8989	6.68	4.61
grass	4	5993	4.46	3.07
shrubs	5	20463	15.22	10.49
aspen	6	11330	8.43	5.81
young lodgepole pine	7	8230	6.12	4.22
mature lodgepole pine	8	78952	58.71	40.48
shadow	10	15639	11.63	8.02
Null	0	42963	31.95	22.03
Image total		195050	145.05	100.00

Table 4.4: Results of the species-based MLC

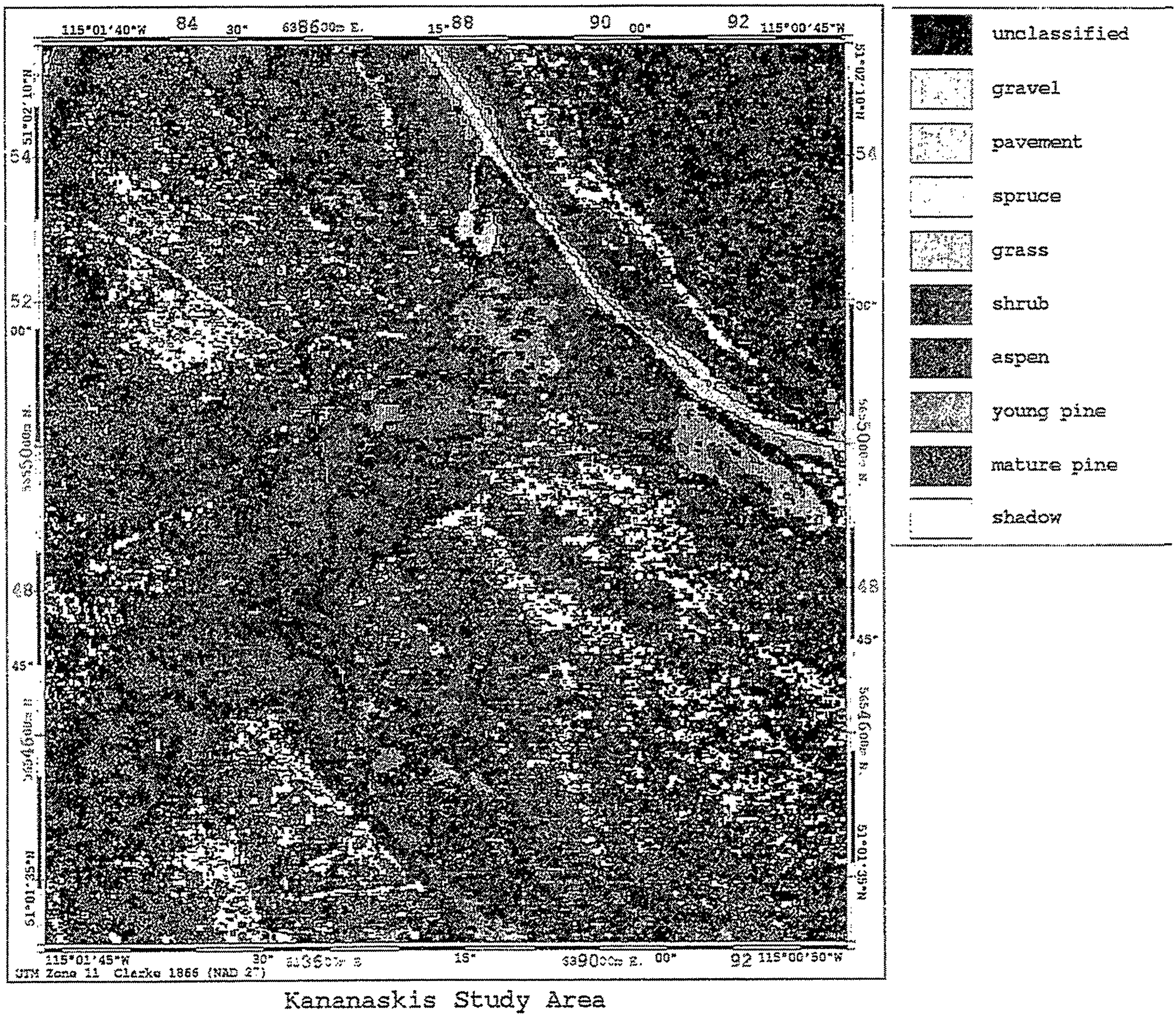

Figure 4.1: Species-based MLC of the Kananaskis study area

4.2.1.2 Dwarf mistletoe classification using *casi* channels

The second classification was performed using the 6 channel subset of the original *casi* channels (see Table 4.3). These 6 channels (520.2nm, 548.6nm, 674.6nm, 743.1nm, 752.1nm, and 772.0nm) were used for an MLC classification designed to separate the dwarf mistletoe-infested lodgepole pine from healthy lodgepole pine. It should be noted

Class	Code	Pixels	Hectares	% Image
pavement	1	1453	.91	.74
gravel	2	1708	1.07	.88
white spruce	3	21855	13.66	11.20
grass	4	9567	5.98	4.90
shrubs	5	28802	18.00	14.77
aspen	6	15346	9.59	7.87
young lodgepole pine	7	9510	5.94	4.88
mature lodgepole pine	8	40277	25.17	20.65
mature lodgepole pine with dwarf mistletoe	9	31004	19.38	15.90
shadow	10	12901	8.06	6.61
Null	0	22627	14.14	11.60
Image total		195050	121.91	100.00

Table 4.5: Dwarf mistletoe classification using the original *casi* channels

that this selection of *casi* channels was not the best selection of channels available, and that the purpose of this classification was to provide a comparison with the classification which was performed using the 6 optimal channels from all the input channels which were evaluated during the image dimension reduction process (Section 4.2.1.3). If the accuracy of the two classifications are comparable, the time savings which would be gained by using only *casi* channels would be substantial and would make this approach very attractive. The results of the classification using the 6 *casi* channels are shown in

Figure 4.2 and Table 4.5. The accuracy of the classification is outlined and discussed in Section 4.3.

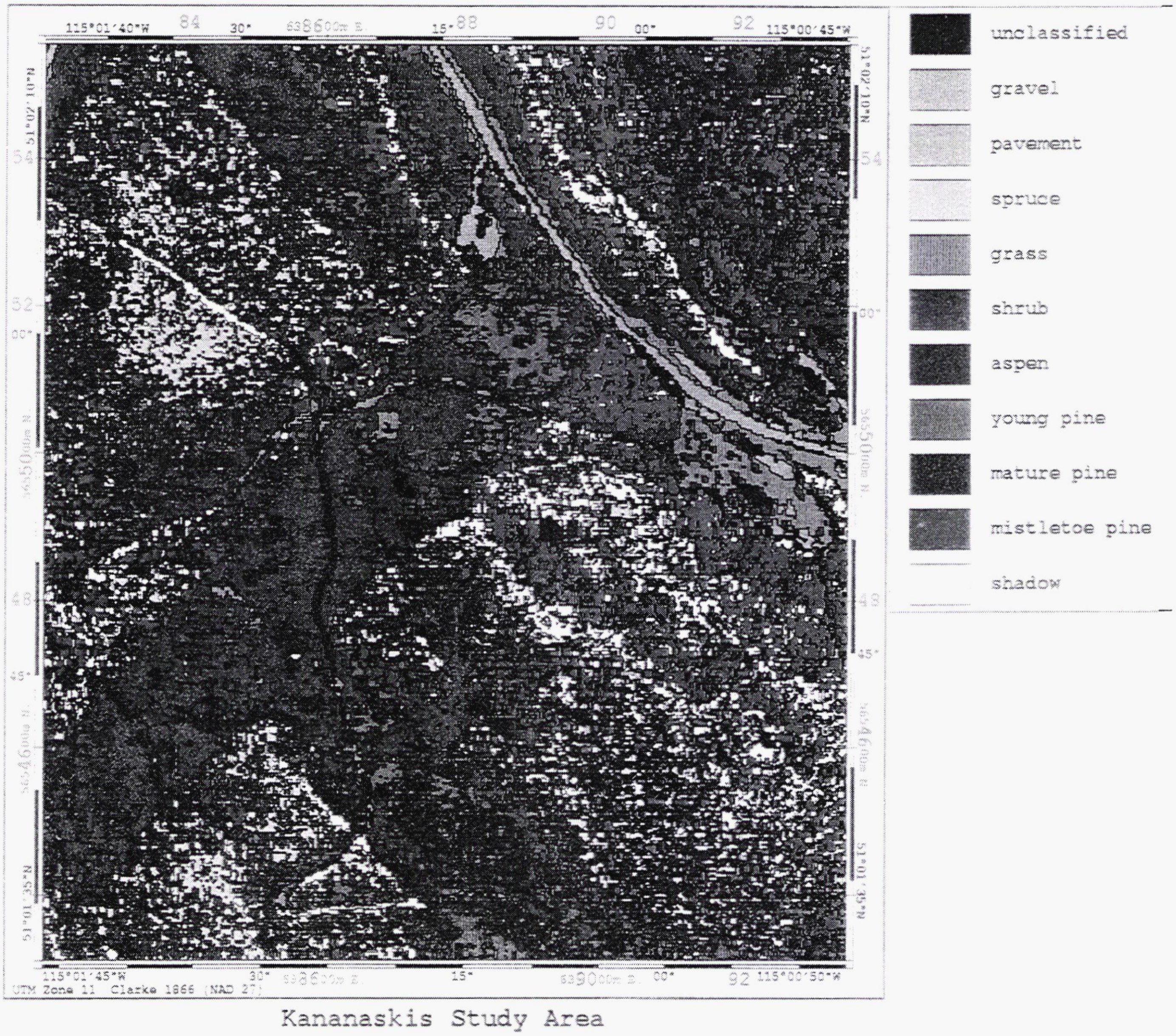

Figure 4.2: Dwarf mistletoe classification using the original *casi* channels

4.2.1.3 Dwarf mistletoe classification using the optimal 6 channels

The third classification was performed using the 6 optimal channels which were selected from the entire set of input channels (520.0nm, 548.6nm, PC3, texture, normalized 487.4nm, normalized 548.6nm - see Table 4.3). This classification, therefore, was intended to be the optimal classification of healthy and dwarf mistletoe-infested lodgepole pine using the available *casi* imagery. The results of this classification are shown in Figure 4.3 and Table 4.6, and the accuracy of the classification is outlined and discussed in Section 4.3.

Class	Code	Pixels	Hectares	%Image
pavement	1	663	.41	.34
gravel	2	1828	1.14	.94
white spruce	3	8776	5.48	4.50
grass	4	5993	3.75	3.07
shrubs	5	20593	12.87	10.56
aspen	6	11330	7.08	5.81
young lodgepole pine	7	7864	4.91	4.03
mature lodgepole pine	8	51636	32.27	26.47
mature lodgepole pine with dwarf mistletoe	9	24178	15.11	12.40
shadow	10	15909	9.94	8.16
Null	0	46280	28.92	23.73
Image total		195050	121.91	100.00

Table 4.6: Optimal dwarf mistletoe separation using the MLC

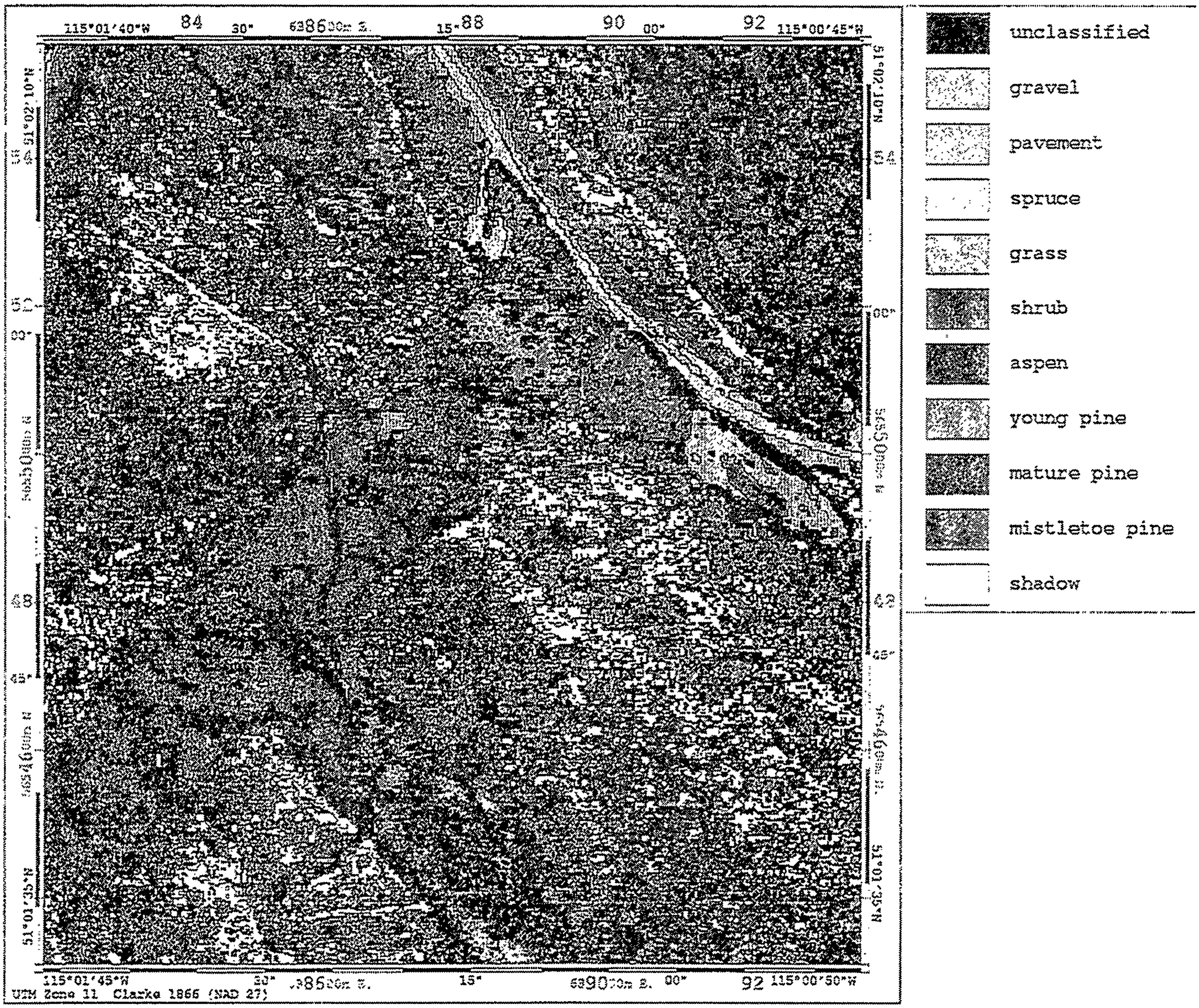

Kananaskis Study Area

Figure 4.3: Optimal dwarf mistletoe separation using the MLC

4.3 DISCUSSION OF KANANASKIS RESULTS

In this Section, the classifications which were produced from the Kananaskis imagery will be discussed. Two accuracy measures were used to assess the accuracy of the classifications which were performed. The first involved an assessment of how accurately the pixels which were used to train the MLC were actually classified. The results of this assessment provided an indication of the quality of the training areas. The use of training pixels for an assessment of the overall classification accuracy creates results which are biased due to the use of the same pixels to both train and assess the accuracy of the classifier. As a result, separate testing areas were developed and used for an assessment of the accuracy the classification results.

4.3.1 Accuracy of species classification

An assessment was made of the accuracy to which the major species in the study area were classified. While the main object of this study was the discrimination of healthy and dwarf mistletoe-infested lodgepole pine, it was worthwhile to use the opportunity to conduct a study of the accuracy of species discrimination using the MLC. Results of the classification are shown in a classification map in Figure 4.1 and in tabular form in Table 4.4. Table 4.7 shows the accuracy of the species-based classification.

The species-based classification produced accurate results with an average accuracy of 84.7%. The largest amount of confusion was found between the three conifer classes. The young lodgepole pine and mature lodgepole pine classes had considerable overlap with 20.4% of the young pine being classified as mature pine and 7.2% of the mature pine classified as young pine. Given that the two classes are the same species of tree this is not surprising and is a reasonably good result. Confusion also existed between the spruce and mature pine with 13.5% of the spruce classified as mature lodgepole pine. This is consistent with the results of other researchers, such as Ekstrand (1994), who also have

Areas		Percent pixels classified by code									
Code	Name	0	1	2	3	4	5	6	7	8	10
1	pavement	4.1	**91.5**	.0	.0	4.4	.0	.0	.0	.0	.0
2	gravel	2.5	.0	**94.4**	.0	3.1	.0	.0	.0	.0	.0
3	spruce	4.7	.0	.0	**70.8**	.0	.0	.0	.0	13.5	11.0
4	grass	5.3	1.9	4.0	.0	**83.2**	5.5	.0	.0	.0	.0
5	shrub	1.6	.0	.0	.0	5.8	**92.2**	.2	.0	.2	.0
6	aspen	12.8	.0	.0	.0	1.5	4.6	**79.5**	1.5	.0	.0
7	young pine	3.2	.0	.0	.0	.0	.9	.0	**75.5**	20.4	.0
8	mature pine	6.7	.0	.0	.3	.0	1.0	.0	7.2	**84.5**	.2
10	shadow	5.0	.0	.0	4.0	.0	.0	.0	.0	.0	**91.0**

Average accuracy = 84.74%

Table 4.7: Accuracy of species-based classification

found overlap between spruce and lodgepole pine. Overall, the results were very favourable.

It should be remembered, however, that the purpose of the channel selection process was to select the channels which highlight the discrimination between healthy lodgepole pine and dwarf mistletoe-infested lodgepole pine, and that better results could probably have been obtained if the channel selection process had been designed to emphasize the separation between all classes.

4.3.2 Accuracy of dwarf mistletoe classification using *casi* channels

This classification was performed using the 6-channel subset of the original *casi* channels (520.2nm, 548.6nm, 674.6nm, 743.1nm, 752.1nm, and 772.0nm) and included a dwarf mistletoe-infested lodgepole pine class. The results are shown in Table 4.3 and Figure 4.2.

4.3.2.1 Accuracy of training area assignment using *casi* channels

In general, the training pixels were classified accurately with an average accuracy of 89.5%. Training pixels for mature lodgepole pine with dwarf mistletoe were classified with an accuracy of over 93%. The mature pine training pixels, however, were classified with an accuracy of only 54.3%. A large percentage of the mature pine training pixels were assigned to the young lodgepole pine, dwarf mistletoe-infested lodgepole pine, spruce, and shadow classes. This result would be of concern if this were the main classification of the project, however, it has already been explained that this selection of *casi* channels was not the best selection of channels available, and that these results will be compared with those resulting from the optimal classification.

Training pixels for the shadow class were assigned with an accuracy of over 88%. The largest misclassification of the shadow class involved the spruce class with 7.2% of the shadow training pixels assigned to the spruce class and 4.8% of the spruce training pixels classified as shadow. The confusion between the spruce and shadow is due to the fact that shadowed areas of other classes exhibit spectra which are similar to the spruce spectra. The results indicate that the shadow training areas were well developed.

All non-conifer training pixels were classified with an accuracy of over 90% indicating that they were accurate representations of the classes.

4.3.2.2 Accuracy of classification using *casi* channels

The accuracy of the classification was assessed using test areas, the results of which are shown in Table 4.9. The overall accuracy of the classification was 81%. Significant confusion was evident among the conifer classes with a mature lodgepole pine classification accuracy of 55%. With respect to the mature lodgepole pine, 20% was classified as young lodgepole pine, 9.5% as dwarf mistletoe-infested lodgepole pine, and

Areas		Percent training pixels classified by code										
Code	Name	0	1	2	3	4	5	6	7	8	9	10
1	pavement	3.1	**93.1**	.0	.0	3.8	.0	.0	.0	.0	.0	.0
2	gravel	3.5	.2	**93.8**	.0	2.5	.0	.0	.0	.0	.0	.0
3	spruce	1.1	.0	.0	**86.6**	.0	.0	.0	.0	7.5	.0	4.8
4	grass	.6	.6	.6	.0	**96.6**	1.5	.0	.0	.0	.0	.0
5	shrub	.2	.0	.0	.0	2.5	**97.0**	.3	.0	.0	.0	.0
6	aspen	1.3	.0	.0	.0	.0	.7	**98.0**	.0	.0	.0	.0
7	young pine	.7	.0	.0	.0	.0	.2	.0	**93.2**	4.6	1.2	.0
8	mature pine	1.4	.0	.0	11.8	.3	.6	.3	21.5	**54.3**	9.9	.0
9	pine with mistletoe	1.2	.0	.0	.0	.2	.0	.0	.7	4.0	**93.6**	.2
10	shadow	4.2	.0	.0	7.2	.0	.0	.0	.0	.2	.0	**88.4**

Average accuracy = 89.47%

Overall accuracy = 84.31%

Kappa Coefficient = 0.82 Standard Deviation = 0.00511

Table 4.8: Accuracy of training area assignment using subset of *casi* channels

8.3% as spruce. This indicates that the class signatures developed using the *casi* channels had significant overlap between conifer classes.

Areas		Percent test pixels classified by code										
Code	Name	0	1	2	3	4	5	6	7	8	9	10
1	pavement	3.1	**93.1**	.0	.0	3.8	.0	.0	.0	.0	.0	.0
2	gravel	3.6	.2	**93.8**	.0	2.4	.0	.0	.0	.0	.0	.0
3	spruce	1.3	.0	.0	**73.4**	.0	.0	.0	.0	17.1	.8	7.4
4	grass	1.1	14.3	3.4	.0	**72.0**	9.1	.0	.0	.0	.0	.0
5	shrub	1.0	.0	.0	.0	2.9	**95.7**	.2	.0	.0	.2	.0
6	aspen	2.1	.0	.0	.0	.5	2.1	**93.8**	1.5	.0	.0	.0
7	young pine	2.1	.0	.0	.0	3.0	2.5	.2	**73.1**	12.5	6.5	.0
8	mature pine	4.8	.0	.0	8.3	.6	.6	.4	20.3	**54.8**	9.5	.6
9	pine with mistletoe	.9	.0	.0	2.0	.0	9.0	.0	.7	15.1	**71.5**	.9
10	shadow	4.2	.0	.0	7.2	.0	.0	.0	.0	.2	.0	**88.4**

Average accuracy = 80.96%

Overall accuracy = 81.19%

Kappa Coefficient = 0.788 Standard Deviation = 0.00625

Table 4.9: Accuracy of classification using subset of original *casi* channels

The dwarf mistletoe-infested lodgepole pine was classified with an accuracy of 71.5% with 15% classified as mature lodgepole pine class. This result is very encouraging and indicates that the two health states of mature lodgepole pine can be separated with a high level of accuracy. A significant portion of the dwarf mistletoe-infested lodgepole pine was classified as shrub (9%) which may be related to the decreased canopy closure of the infested stands which would expose more understory and therefore result in similar spectra to shrubs.

The shadow class was classified well with an accuracy of 88.4% which indicates that it is demarcating a class which is distinct from the other classes.

Areas		Percent training pixels classified by code										
Code	Name	0	1	2	3	4	5	6	7	8	9	10
1	pavement	4.1	**91.5**	.0	.0	4.4	.0	.0	.0	.0	.0	.0
2	gravel	2.5	.0	**94.3**	.0	3.2	.0	.0	.0	.0	.0	.0
3	spruce	1.3	.0	.0	**83.9**	.0	.0	.0	.0	7.2	.0	7.5
4	grass	.6	.3	1.8	.0	**92.0**	5.2	.0	.0	.0	.0	.0
5	shrub	.1	.0	.0	.0	1.5	**97.6**	.8	.0	.0	.0	.0
6	aspen	.0	.0	.0	.0	.2	1.8	**98.0**	.0	.0	.0	.0
7	young pine	1.0	.0	.0	.0	.0	.0	.0	**93.9**	3.7	1.5	.0
8	mature pine	3.0	.0	.0	5.1	.0	.1	.0	15.6	**67.5**	8.0	.8
9	pine with mistletoe	1.6	.0	.0	.0	.0	.0	.0	.2	5.4	**92.5**	.2
10	shadow	5.0	.0	.0	4.0	.0	.0	.0	.0	.0	.0	**91.0**

Average accuracy = 90.23%

Overall accuracy = 87.48%

Kappa Coefficient = 0.856 Standard Deviation = 0.0047

Table 4.10: Accuracy of training pixel assignment for optimal classification

4.3.3 Accuracy of classification using the optimal 6 channels

In the following Sections, the classification which was performed using the 6 optimal channels from the channel selection process (520.0nm, 548.6nm, PC3, Texture, normalized 487.4nm, normalized 548.6nm - see Table 4.3) will be discussed. As this classification used the 6 optimal channels which were selected for the highest discrimination of mature healthy and dwarf mistletoe-infested lodgepole pine, it should result in the most accurate classification in terms of mature lodgepole pine classes using the available imagery. The results of this classification will be compared to the classification performed using the subset of *casi* channels to determine if any improvement in accuracy was gained from the inclusion of the image enhancements.

4.3.3.1 Training area accuracy using optimal channels

Table 4.10 indicates that the training area pixels were well classified with an average accuracy of over 90%. The lowest accuracy involved the healthy lodgepole pine class which had misclassification errors with young lodgepole pine (15.6%) and dwarf mistletoe-infested lodgepole pine (8%). Again, this result is not surprising since the three classes are the same species, and as a result, have very similar spectra.

The shadow training pixels were again assigned very well with an accuracy of 91% indicating that the shadow training areas represented a distinct class. All non-conifer training pixels were classified very well with accuracies in excess of 90%.

4.3.3.2 Accuracy of optimal classification

The average accuracy obtained using the 6 optimal channels was 84.6% (Table 4.11) compared to an 81% accuracy using only *casi* channels. Confusion was highest among the conifer classes with mature lodgepole pine classified with an accuracy of 75% and dwarf mistletoe-infested lodgepole pine classified with an accuracy of 61.8%. Dwarf mistletoe-infested lodgepole pine had a 23.7% misclassification error with healthy lodgepole pine and had 12% improperly assigned to the null class indicating that confusion still exists between the two mature lodgepole pine classes. The error in classification may be caused by variations in the severity of dwarf mistletoe-infestation which would result in a range of spectral changes in infested areas making absolute distinction difficult. Lightly infested lodgepole pine would have a similar spectral response to healthy lodgepole pine. As this was an initial study on dwarf mistletoe, no assessment was made of the severity infestation and this is an important topic for future studies.

Areas		Percent test pixels classified by code										
Code	Name	0	1	2	3	4	5	6	7	8	9	10
1	pavement	4.1	**91.5**	.0	.0	4.4	.0	.0	.0	.0	.0	.0
2	gravel	2.5	.0	**94.3**	.0	3.2	.0	.0	.0	.0	.0	.0
3	spruce	5.1	.0	.0	**70.0**	.0	.0	.0	.0	12.9	0.8	11.2
4	grass	.6	.3	1.8	.0	**92.0**	5.2	.0	.0	.0	.0	.0
5	shrub	.1	.0	.0	.0	1.5	**97.6**	.8	.0	.0	.0	.0
6	aspen	.0	.0	.0	.0	.2	1.8	**98**	.0	.0	.0	.0
7	young pine	5.1	.0	.0	.0	.0	.9	.0	**74.5**	14.1	5.3	.0
8	mature pine	6.0	.0	.0	.0	.0	.0	.0	11.4	**75.1**	6.8	.2
9	pine with mistletoe	12.1	.0	.0	.0	.0	2.0	.0	.0	23.7	**61.8**	0.4
10	shadow	5.0	.0	.0	4.0	.0	.0	.0	.0	.0	.0	**91.0**

Average accuracy = 84.60%

Overall accuracy = 86.74%

Kappa Coefficient = 0.849 Standard Deviation = 0.005

Table 4.11: Accuracy of optimal classification

The combined average accuracy of the mature lodgepole pine and the dwarf mistletoe-infested lodgepole pine classes was 68.5% which was 5.35% higher than that attained using only the *casi* channels (Table 4.9) indicating that the texture and other image enhancements provided valuable information for discriminating between the mature lodgepole pine classes. All non-conifer classes were classified with an accuracy of over 90% due to the fact that they are much more distinct classes than the conifer classes as was indicated during field spectrometer tests.

The results indicate that dwarf mistletoe-infested lodgepole pine can be distinguished from healthy lodgepole pine using *casi* imagery. While there was confusion between conifer classes, the accuracy of the dwarf mistletoe-infested lodgepole pine classification indicates that the *casi* has much potential as a tool for mapping dwarf mistletoe on lodgepole pine. The accuracies attained in this study would be sufficient to provide an outline of the location of dwarf mistletoe infestations which would allow for further assessment by ground surveys. Further research into this area would likely improve the distinction between the healthy and dwarf mistletoe-infested lodgepole pine.

5. CONCLUSIONS AND RECOMMENDATIONS

In this chapter, a summary of this project is provided along with conclusions and recommendations for further study.

5.1 SUMMARY

The primary objective of this project was to determine the applicability of the Compact Airborne Spectroscopic Imager (*casi*) for distinguishing between healthy and dwarf mistletoe-infested lodgepole pine. Dwarf mistletoe is one of the most serious threats to lodgepole pine in western Canada and the United States and results in significant reductions in forestry yield in infested areas. Accurate, efficient assessment of the extent of dwarf mistletoe infestation is required to improve control. Present methods for assessment are very subjective and are not extremely accurate. One factor which is repeatedly mentioned by researchers is the lack of accurate data on the extent of dwarf mistletoe infestation (e.g. Baker, 1992). In this Section, the process which was followed during this project to assess the use of *casi* imagery for identifying dwarf mistletoe on mature lodgepole pine is summarized.

An analysis of the physiology and life-cycle of lodgepole pine dwarf mistletoe was conducted to acquire information to assist in the analysis of dwarf mistletoe using *casi* imagery. A study area was then identified which had stands of healthy and dwarf mistletoe-infested lodgepole pine. *Casi* imagery was then collected for the study area. The spectral characteristics of healthy and dwarf mistletoe-infested lodgepole pine as well as the other major species in the study area were examined using a hand-held spectrometer which revealed that differences existed which should allow for the discrimination of the different classes. When compared to healthy lodgepole pine, the dwarf mistletoe-infested lodgepole pine was found to exhibit higher reflectance in all wavelengths which were sampled. The largest difference was evident in the near-infrared wavelengths with infested lodgepole pine having a reflectance which was approximately 6% higher than the healthy lodgepole pine. Significant differences were also found in the visible wavelengths with the significant increases in reflectance found in the green and red wavelengths. A small blue shift of the red edge (approximately 5 nm) was also evident which has been correlated in other studies with decreased plant health (i.e. Essery and Morse, 1992).

Based on the analysis of the field spectrometer results, band selection for a classification intended to differentiate between mature healthy and dwarf mistletoe-infested lodgepole pine should emphasize the NIR wavelengths (750-850nm) and the peak of green reflectance (~550nm). Additional channels should be selected from the area of the spectrum between the upper portion of the green wavelengths and the middle portion of the red wavelengths (550-650nm) as well as the lower portion of the green wavelengths (500-550nm), both regions in which small differences were evident in the field spectra of lodgepole pine. The red edge was also identified as having the potential for providing important information for discriminating between healthy and dwarf mistletoe-infested mature lodgepole pine.

Following field spectrometer studies, a number of image enhancements, including band combinations, band ratios, and band transformations, which were designed to provide information for discriminating between healthy and dwarf mistletoe-infested lodgepole pine, were then completed. An optimization procedure was developed and implemented to reduce the dimensionality of the data set and to select the optimal set of *casi* bands and image enhancements to best distinguish between healthy and dwarf mistletoe-infested lodgepole pine using the available *casi* imagery. Two channel sets were then produced - the first was a 6 channel subset of all input channels including *casi* channels and image enhancements. This optimal channel set consisted of channels containing the following information: texture, PC3, normalized 487.4nm, normalized 548.6nm, and two *casi* channels - 520.0nm and 548.6nm.

The second channel set was derived only from *casi* channels and consisted of channels centered at 520.2nm, 548.6nm, 674.6nm, 743.1nm, 752.1nm, and 772.0nm. This subset of channels was used to create a classification which was analysed to determine if any improvement in classification accuracy was gained by using the image enhancements which were included in the optimal channel set.

The maximum-likelihood classifier was then used to classify the imagery and the accuracy of the classifications was then subsequently determined. Two classifications designed to distinguish between mature healthy and dwarf mistletoe-infested lodgepole pine were performed. The first was performed using the optimal channel set and the resultant classification achieved an average accuracy of 68.5 % for the healthy and dwarf mistletoe-infested mature lodgepole pine classes. The second classification was performed using the *casi* channel subset and resulted in an average accuracy of 63 % for the healthy and dwarf mistletoe-infested lodgepole pine classes indicating that the texture and other image enhancements provided valuable information for discriminating between the mature lodgepole pine classes.

5.2 CONCLUSIONS

Based on the results of this project, the following conclusions can be made:

1. Lodgepole pine dwarf mistletoe produces physiological effects which result in changes in the spectra of infested trees. The spectral changes include increased NIR reflectance, a blue shift of the red edge, and increased reflectance in the visible wavelengths, particularly in the green and red wavelengths;

2. Classification results indicated that it is possible to discriminate between healthy and dwarf mistletoe-infested mature lodgepole pine. A classification accuracy of

63% was attained using a 6 channel subset of *casi* channels which consisted of the following channels: 520.2nm, 548.6nm, 674.6nm, 743.1nm, 752.1nm, and 772.0nm;

3. The level of discrimination of dwarf mistletoe can be increased through the inclusion of image enhancements including textural information, the 3rd principal component and normalized *casi* channels. The classification accuracy for healthy and dwarf mistletoe-infested mature lodgepole pine was increased to 68.5% using a 6 channel set consisting of: texture, PC3, normalized 487.4nm, normalized 548.6nm, and two *casi* channels - 520.0nm and 548.6nm.

5.3 RECOMMENDATIONS

This study has indicated that *casi* imagery has the potential to serve as a tool for the identification of lodgepole pine dwarf mistletoe and that further research should be conducted in a number of areas to improve the discrimination of dwarf mistletoe-infested lodgepole pine. As this was an initial study on lodgepole pine dwarf mistletoe, the emphasis was placed on ensuring that any differences in lodgepole pine spectra were due to dwarf mistletoe and not other factors. This was achieved by selecting a site where the lodgepole pine had no other insect or disease damage and where site conditions such as soil type and moisture levels were relatively consistent. As a result, additional study should be conducted to determine the influence of other factors such as soil conditions, moisture levels, topography, wind, and seasonal variations on the spectra of lodgepole pine and the resultant classification using *casi* imagery. In addition, future studies could look into the possibility of distinguishing between different levels of severity of dwarf mistletoe infestation and should also examine the question of whether dwarf mistletoe is differentiable from other lodgepole pine diseases or pests.

The development of accurate tree isolation algorithms would greatly increase the applicability of using mid or high resolution multispectral imagery for dwarf mistletoe detection. Areas not identified as trees could then be eliminated from further analysis. In addition, accurate training areas could then be developed containing pure samples of each class which would greatly reduce the confusion between classes and improve the accuracy of estimates of the extent of dwarf mistletoe infestation.

Field spectrometer studies revealed that significant differences exist in the spectra of healthy and dwarf mistletoe-infested young lodgepole pine. Based on this data, future studies should attempt to discriminate between healthy young lodgepole pine and dwarf mistletoe-infested young lodgepole pine using high resolution multispectral imagery. Such a process would require the use of imagery with a resolution of less than 1 meter to allow for the isolation of the young lodgepole pine which have crowns which range in size from approximately 0.5 m^2 to 2 m^2. Young lodgepole pine are most susceptible to serious damage from dwarf mistletoe as the disease affects their early growth. In addition, the pathogen then has a longer period over which to affect the tree such that many trees infested at a young age will never be suitable for harvest. The identification of dwarf mistletoe in young lodgepole pine would allow for control measures to be taken such as destroying both the infested young lodgepole pine and the source of the dwarf mistletoe and replanting new trees.

The inclusion of a digital elevation model (DEM) should be investigated to reduce the classification error between the spruce class and the other conifers. A DEM would provide valuable discriminatory information because the location of the various conifers is highly influenced by aspect and elevation.

The advent of mid and high spatial and spectral resolution satellite imagery over the next few years should greatly expand the use of high resolution imagery for forest health assessment. Once available, such imagery should be studied for the purpose of developing widescale inventories of lodgepole pine dwarf mistletoe.

REFERENCES

Agrios, G.N. "Plant Pathology", *Academic Press*, Inc., Toronto, 1986.

Babey, S.K., and Soffer, R.J. "Radiometric Calibration of the Compact Airborne Spectrographic Imager (CASI)", *Canadian Journal of Remote Sensing*, vol. 18, no. 4, October, 1992, pp. 233-242.

Babey, S.K., and Anger C.D. "Compact airborne spectrographic imager (CASI): a Progress Review", Presented at the *SPIE Conference*, Orlando, Florida, April, 1993, 12 p.

Baker, F.A., Knowles, K. Slivitsky, M. "Impact of Dwarf Mistletoe on Jack Pine Forests in Manitoba", *Plant Disease,* vol. 76, no. 12, 1992, pp. 1256-1258.

Blackburn, G.A., and Milton, E.J. "An Application of Airborne Imaging Spectrometry to Ecological Studies of Woodlands", Presented at the *First International Airborne Remote Sensing Conference and Exhibition*, Strasbourg, France, September, 1994, pp. 382-393.

Brandt, J.P., "Forest insect and disease conditions in west-central Canada in 1993 and predictions for 1994", *Information Report NOR-X-335*, Northern Forestry Centre, 1994.

Brandt, J.P. Amirault, R. "Forest insect and disease-caused depletions to forest of west-central Canada-1982-1987.", *Information Report NOR-X-333*, Northern Forestry Centre, 1994.

Chapman, M.A., Stoness, A.J. "Assessment of infrared photography for dwarf mistletoe identification", *unpublished report*, 1995.

Cohen, W.B. "Response of Vegetation Indices to Changes in Three Measures of Leaf Water Stress", *Photogrammetric Engineering and Remote Sensing*, vol. 57, no. 2, 1991, pp. 195-201.

Cosandier, D., Ivanco, T., and Mah, S. "The Geocorrection and Integration of the Global Positioning System with the Compact Airborne Spectrographic Imager", Presented at the 15th *Canadian Symposium on Remote Sensing*, June, 1992, pp. 385-390.

Cosandier, D., Chapman, M.A., and Ivanco, T. "Low Cost Attitude Systems for Airborne Remote Sensing and Photogrammetry", Presented at *The Canadian Conference of GIS*, Ottawa, March, 1993, 8 p.

Cosandier, D., Ivanco, T., and Chapman, M.A. "The Integration of a Digital Elevation Model in casi Image Geocorrection", Presented at the *First International Airborne Remote Sensing Conference and Exhibition*, Strasbourg, France, 1994, 17 p.

Ekstrand, S. "Use of CASI for Forest Damage Monitoring", Presented at the *First International Airborne Remote Sensing Conference and Exhibition*, Strasbourg, France, September, 1994, pp. 205-213.

Essery, C.I., Morse, A.P., "The impact of ozone and acid mist on the spectral reflectance of young Norway spruce trees", International Journal of Remote Sensing, 1992, pp. 3045-3053.

Forestry Canada, "Forestry Leaflet 18: Dwarf mistletoe", Ministry of Supply and Services Canada, 1992.

Franklin, S.E., Bowers, W.W., and Ghitter, G. "Discrimination of adelgid-damage on single balsam trees with aerial remote sensing data", Draft manuscript, 1994, 37 p.

Franklin, S.E. and McDermid, G.J. "Empirical relations between digital SPOT HRV and CASI spectral response and lodgepole pine (Pinus contorta) forest stand parameters", *International Journal of Remote Sensing*, 1993, vol. 14, no. 12, pp. 2331-2348.

Franklin, S.E., and Raske, A.G. "Satellite Remote Sensing of Spruce Budworm Forest Defoliation in Western Newfoundland", *Canadian Journal of Remote Sensing*, vol. 20, no. 1, 1994, pp. 37-48.

Freemantle, J.R., Pu, R., Miller, J.R. "Calibration of imaging spectrometer data to reflectance using pseudo-invariant features", Draft of paper presented at; *15th Canadian Symposium on Remote Sensing*, June, 1994, 7 p.

Gemmell, F.M., Colls, J.J. "The effects of sulphur dioxide on the spectral characteristics of leaves of vicia faba L.", International Journal of Remote Sensing, Vol. 13, No. 14, 1992, pp. 2547-2563.

Gong, P., Remote Sensing and Image Analysis. Lecture notes, Department of Geomatics Engineering, The University of Calgary, ENGO 655, Remote Sensing and Image Analysis, 1993.

Gougeon, F.A., "Individual Tree Identification from High Resolution MEIS Images", Proceedings of the *International Forum on Airborne Multispectral Scanning for Forestry and Mapping (with emphasis on MEIS)*, Val-Morin, April, 1992, pp. 117-128.

Gunther, K.P., Dahn, H.G., Ludeker, W., "Remote Sensing of Vegetation Status by Laser-Induced Fluorescence", *Remote Sensing of Environment*, 1994, pp. 10-17.

Hall, J.P. "Forest Insect and Disease Conditions in Canada 1992", *Information Report NOR-X-322*, Northern Forestry Centre, Ottawa, 1994.

Harron, J.W., Freemantle, J.R., Hoolinger, A.B., and Miller, J.R. "Methodologies and Errors in the Calibration of A Compact Airborne Spectrographic Imager", Draft of paper presented at the *15th Canadian Symposium on Remote Sensing*, Toronto, June, 1992, 7p.

Held, A.A., and Jupp, D.L.B. "Use of the Compact Airborne Spectral Imager (CASI) for Remote Sensing of Vegetation Function and Dynamics", Presented at the 7^{th} *Australian Remote Sensing Conference*, Melbourne, Australia, 1994, 8p.

Hiratsuka, Y. "Forest tree diseases of the prairie provinces", *Information Report NOR-X-286*, Northern Forestry Centre.

Horsfall, J.G., Cowlin, E.B., "Plant Diseases", *Academic Press*, Ltd., Toronto, 1977.

Hord, M., "Remote Sensing; Methods and Applications", John Wiley & Sons, Inc., New York, 1986.

Hudak, J., Franklin, S.E., and Luther, J.E. "Detection and Classification of Forest Damage Using Remote Sensing", Proceedings of the *International Forum on Airborne Multispectral Scanning for Forestry and Mapping (with emphasis on MEIS)*, Val-Morin, April, 1992, pp. 36-44.

Jakubauskas, M.E., "Image Texture Analysis of Coniferous Forest Successional Stages", *Remote Sensing of Environment*, 1993, pp. 272-279.

Jensen, J.R., "Introductory Digital Image Processing", *Prentice Hall*, New Jersey, 1986.

Leckie, D.G., "Application of Airborne Multispectral Scanning to Forest Inventory Mapping", Proceedings of the *International Forum on Airborne Multispectral Scanning for Forestry and Mapping (with emphasis on MEIS)*, Val-Morin, April, 1992, pp. 86-93.

Malthus, T.J., Madeira, A.C., "High Resolution Spectroradiometry: Spectral Reflectance of Field Bean Leaves Infected by Botytis fabae", *Remote Sensing of Environment*, vol. 45, 1993, pp. 107-116.

McArdle, S.S., Miller, J.R., and Freemantle, J.R. "Airborne Image Acquisition Under Cloud: Preliminary Comparisons With Clear-Sky Scene Radiance and

Reflectance Imagery", Draft of paper presented at the *15th Canadian Symposium on Remote Sensing*, Toronto, June, 1992, 8p.

McQueen, D.A., Punter, D. "Floral Biology of Dwarf Mistletoe in Manitoba", *Interim Report submitted to Forestry Canada*, June, 1994, 3 p.

Murtha, P.A., "Considerations for Forest Health/Damage Assessment with MEIS", Proceedings of the *International Forum on Airborne Multispectral Scanning for Forestry and Mapping (with emphasis on MEIS)*, Val-Morin, 1992, pp. 46-53.

O'Connor, M.C., Wells, E.D., Luther, J.E., and Franklin, S.E. "Reflectance measurements of species and cover on prescribed burn sites in western Newfoundland", Poster paper, *17th Canadian Symposium on Remote Sensing*, Saskatoon, June, 1995, 5p.

PCI, INC., "EASI/PACE Version 5.3 Reference Manuals", Richmond Hill, 1994.

Punter, D., Gilbert, J., "Animal vectors of Arceuthobium Americanum seed in Manitoba", *Canadian Journal of Forest Research*, vol. 19, 1989, pp. 805-809.

Reinartz, P., "Classification of Forest Damages in Germany with Airborne Multispectral Data", Proceedings of the *International Forum on Airborne Multispectral Scanning for Forestry and Mapping (with emphasis on MEIS)*, Val-Morin, April, 1992, pp. 54-58.

Shepherd, P.R., and Xu, Q.F. "An Error Analysis of A Reflectance Conversion Methodology Using An Irradiance Sensor", *16th Canadian Symposium on Remote Sensing*, 1993, pp. 851-856.

Staenz, K. "A Decade of Imaging Spectrometry in Canada", *Canadian Journal of Remote Sensing*, vol. 18, no. 4, October, 1992, pp. 187-197.

Staenz, K. "Development of Imaging Spectrometry in Canada", Draft of paper presented at the *International Symposium on Spectral Sensing Research (ISSSR)*, Maui, Hawaii, November, 1992, 14p.

Steiner, T.E., Davidson, A.G., "Forest Insect Conditions", Forestry Canada, 1981.

Wang, L., He, D.C., "A New Statistical Approach For Texture Analysis", *Photogrammetric Engineering and Remote Sensing,* Vol. 56, No.1, January, 1990, pp. 61-66.

Wanner, J.L., Tinnin, R.O., "Some effects of infection by Arceuthobium Americanum on the population dynamics of Pinus contorta in Oregon", *Canadian Journal of Forest Research*, vol. 19, 1989, pp. 736-742.

Williams, D.J., Royer, A., O'Neil, N.T., Achal, S., Weale, G. "Reflectance Extraction From CASI Spectra Using Radiative Transfer Simulations and a Rooftop Irradiance Collector", *Canadian Journal of Remote Sensing*, vol. 18, no. 4, October, 1992, pp. 251-261.

Xu, Q.F., O'Neil, N.T., Royer, A., Shepherd, P.R., Teillet, P.M., Williams, D.J., Tarussov, A. "Reflectance Extraction over a Forestry Site Using the Compact Airborne Spectrographic Imager", *16th Canadian Symposium on Remote Sensing*, 1993, pp. 851-856.

Xu, Q.F., O'Neil, N.T., Royer, A., Shepherd, P.R., Teillet, P.M., Williams, D.J., Tarussov, A. "Reflectance Extraction over a Forestry Site Using the Compact Airborne Spectrographic Imager", *16th Canadian Symposium on Remote Sensing*, 1993, pp. 851-856.